Birch *et al. Fire Ecology* (2026) 22:103
https://doi.org/10.1186/s42408-026-00510-7

Fire Ecology

ORIGINAL RESEARCH

Open Access

Post-wildfire effects, fuel dynamics, and overstory structural changes create risks to forest carbon in future fires

Joseph D. Birch[1,2,6*], Matthew B. Dickinson[3], Eric E. Knapp[4], Carol Ewell[5] and Jessica R. Miesel[1,2,6]

Abstract

Background Forest composition and fuel loadings govern wildfire behavior and effects, influencing the vulnerability of forest carbon (C) to emission; however, key uncertainties remain regarding post-fire forest and fuel dynamics and their consequences for C vulnerability to subsequent burns. The objectives of this study were to investigate (1) how forest structure before and after fire compares to the historic natural range of variability; (2) how immediate fire effects and environmental characteristics influence patterns of change in forest structure and biomass over time after fire; and (3) how fire changes forest C vulnerability to emission in future wildfires. We leveraged a unique dataset comprised of nearly immediate (within days) pre- and post-fire forest and fuels measurements in combination with remeasurements spanning a chronosequence of 1–20 years after wildfire in mixed-conifer forests in California, USA.

Results Fire caused enduring reductions in overstory tree densities (50 ± 14%) and increased height to live crown (+ 2.5 ± 0.7 m) thereby shifting forest structure towards the natural range of variability. However, surface fuels rapidly accumulated in the decade after wildfire and standing dead tree biomass increased 249 ± 24% relative to the pre-fire condition and represented 27 ± 3% of all potential fuels. Coarse woody fuels accumulated to pre-fire loadings within 5–7 years after wildfire and accumulation was greatest in forests that burned at high severity. The proportion of aboveground ecosystem C contained within all potential fuels increased from 38 ± 2 to 52 ± 3% over time, indicating an increased vulnerability of forest C to emission with future fire.

Conclusions Fire-mediated increases in height to live crown and decreases in tree density should improve forest resilience to future fires; however, the structural changes were concomitant with increases in standing dead trees and other fuels that are vulnerable to future emission in future fires. After an initial wildfire in long-unburned forests, as was typical in our study sites, repeated low-intensity fires may help to protect large live trees by consuming remaining and re-accumulated fuels, thereby maintaining forest C sink potential and minimizing C pulses from future fires.

Keywords Wildfire, Fire effects, Burn severity, Carbon emissions, Forest change, Fire behavior assessment team

Resumen

Antecedentes La composición del bosque y las cargas de combustible gobiernan el comportamiento y efectos de los fuegos de vegetación, influenciando la vulnerabilidad del carbono forestal (C) hacia la producción de emisiones. Sin embargo, algunas incertidumbres claves permanecen irresueltas en relación a la dinámica del bosque y los

*Correspondence:
Joseph D. Birch
jdcooper@uidaho.edu
Full list of author information is available at the end of the article

combustibles en el post-fuego y sus consecuencias en la vulnerabilidad del C en quemas subsecuentes. Los objetivos de este estudio fueron investigar: 1) cómo la estructura forestal antes y después de un incendio se compara con el rango histórico natural de variabilidad; 2) cómo los efectos inmediatos del fuego y las características ambientales influencian los patrones de cambio en la estructura y biomasa forestal en el tiempo luego de in incendio; y 3) Cómo el fuego cambia la vulnerabilidad del C forestal hacia las emisiones de futuros incendios. Impulsamos el uso de un único conjunto de datos de bosques y combustibles comprendiendo el período casi inmediato (dentro de pocos días) entre el pre-fuego y el post fuego en combinación con la remedición de esos datos en una crono-secuencia que se extendió entre 1 y 20 años luego del incendio en bosques mixtos de coníferas en California, EEUU.

Resultados El incendio causó reducciones duraderas en la densidad de los doseles (50 ± 14%) e incrementó la altura de la copa viva (+ 2.5 ± 0.7 m), modificando la estructura forestal hacia lo que se estima el rango natural de variabilidad. Por supuesto, los combustibles superficiales se acumularon rápidamente en la década post incendio y la biomasa de los árboles muertos en pié se incrementó en un 249 ± 24% en relación a las condiciones del pre fuego, y representaron 27 ± 3% del total de los potenciales combustibles. Los combustibles gruesos se acumularon a cargas equivalentes al pre-fuego entre 5 y 7 años post fuego, y esa acumulación fue mayor en bosques se quemaron a alta severidad. Con el tiempo, la proporción de C contenido en el ecosistema aéreo dentro de todos los potenciales combustibles se incrementó del 38 ± 2% al 52 ± 3%, indicando una vulnerabilidad incremental de emisiones de C del bosque en un futuro incendio.

Conclusiones Los incrementos en altura de la copa viva y el decremento en la densidad de árboles mediados por el fuego, debieran incrementar la resiliencia del bosque a futuros incendios. Sin embargo, los cambios estructurales fueron concomitantes con el incremento de los árboles muertos en pié y otros combustibles que son vulnerables a emisiones en futuros fuegos. Luego de un incendio inicial en bosques sin incendios previos por mucho tiempo, como es típico en nuestros sitios de estudios, la repetición de fuegos de baja intensidad pueden ayudar a proteger grandes árboles vivos mediante el consumo de combustibles que permanecieron en el lugar y/o que se re-acumularon en el tiempo, manteniendo así el potencial del bosque como un almacén de C y minimizando los pulsos C en futuros incendios.

Introduction

As wildfires become more severe under warming and more variable climate (Turco et al. 2023), understanding the processes driving variability in forest outcomes will be crucial to preserving stressed and marginal forests (Hill et al. 2023). Forest resilience (the rate and extent of recovery to pre-disturbance conditions; Pimm 1984) may be impaired when forests experience extreme wildfire behavior or effects, driven by combinations of unnatural stand density, extreme fire weather, and concurrent drought and beetle disturbances (Abatzoglou and Williams 2016; Stevens-Rumann et al. 2018; Dodge et al. 2019; Stephens et al. 2022). Recent fires in California have surpassed the natural range of variability (NRV) in terms of total acres of high fire severity and size of high-severity patches (Ayars et al. 2023), impairing the resilience of these forests (Serra-Diaz et al. 2018). Diminished forest resilience to wildfire may degrade ecosystem services, such as carbon (C) sequestration or habitat quality, and lead to conversion to alternative stable states, such as shrublands (Johnstone et al. 2016; Steel et al. 2023).

Managing forests for enhanced resilience to wildfire requires understanding the fire effects and processes that drive forest change and fuel accumulation. Fires characteristic of the NRV for mixed-severity fire regimes (i.e., pre-Euro-American settlement) maintained relatively low fuel loads and forest densities and promoted forest structures that were resilient to fire and resistant to bark beetle attacks (Parsons and DeBenedetti 1979; Taylor and Skinner 2003). However, loss of Indigenous fire stewardship combined with a history of fire suppression and other land management practices have resulted in forest densification and shifts toward fire-intolerant species such as *Abies* spp. at the expense of *Pinus* and other more fire-adapted taxa (Steel et al. 2015; Brodie et al. 2023). These shifts in forest structure and composition may increase tree competition for water and induce greater susceptibility to drought, bark beetles, or more severe fire effects owing to compounding disturbances and stress (Safford and Stevens 2017; Restaino et al. 2019; Hagmann et al. 2021). As fire inevitably returns to these NRV-departed forests, the dynamics of post-fire mortality and biomass accumulation will influence future fire behavior and effects via the influence of live and dead forest biomass potentially available for consumption (i.e., forest fuels). Thus, forest resilience to future disturbances will depend, in part, upon how forest structure, composition, and fuels change after a fire, and the extent to which forests can avoid undergoing conversion to non-forest conditions. Although most research on forest-to-shrub type conversion has focused on shifts in dominant vegetation composition and structure (Steel et al. 2023), in fire-prone forests the live and dead biomass components together may provide further insights on risks to ecosystem resilience, especially considering compound disturbances. Despite its importance to future fire risk and potential fire behavior, information on the processes and rates governing fuel accumulation after a given fire remains limited.

In California mixed-conifer forests, fuels are an important driver of fire effects (Steel et al. 2015; Miesel et al. 2018; Birch et al. 2023), along with weather and topography. However, consumption by fire is frequently unequal across types of fuels (e.g., downed wood, litter, or canopy fuels; Birch et al. 2023), and the remaining fuel mass and arrangement—and their change over time—may in turn influence the behavior and effects of subsequent fires. For example, a site with a high proportion of fine woody fuels may promote greater energy release by flaming combustion (relative to smoldering combustion), compared to sites with a relatively greater proportion of coarse woody fuels and duff (Rein 2016). Because fuels accumulate through different processes and rates (e.g., branch deposition for 1-h fuels versus litter decomposition for duff), the amount of fuel will depend on time and type of initial fire effects. For example, high severity crown fire may result in a slower accumulation of canopy fuels, litter, and duff, relative to a low-severity surface fire, owing to greater consumption of canopy fuels (Hall et al. 2006; Thompson et al. 2017). Therefore, details about fuel accumulation by class after wildfire may have important implications for fire behavior and C emissions in subsequent fires, ultimately influencing longer-term recovery of forests and forest C stability (Prichard et al. 2010; Williams et al. 2016).

Wildfire-induced forest C release occurs via emissions of C-based gaseous and particulate products of combustion. Wildfire emissions contribute to positive feedback with warmer, drier, and longer fire seasons, which has contributed to a doubling of area burned in the western US between 1979 and 2015 (Abatzoglou and Williams 2016). Even greater increases in area burned and in the patch size of areas burned at high severity are expected, exacerbated by the interaction between longer, drier fire seasons (Clarke et al. 2022) and climate-driven shifts in vegetation (Liu and Wimberly 2016). However, area burned is not the only factor that influences C emissions; the amount and distribution of biomass influences the vulnerability of forest C to loss during fire. For example, in addition to fire directly causing forest C loss, fire-induced mortality of live trees converts C from live to dead biomass pools, thereby increasing the likelihood of fuel consumption—and C emission—in future wildfires. Therefore, the ability to manage forests for increased C stability and sustain their C uptake potential depends on improved knowledge of C distribution among forest pools which affect vulnerability to consumption during future fire.

To explore the processes underlying post-fire fuel accumulation and C vulnerability to future fire, we leveraged existing nearly immediate pre-fire and post-fire measurements of forest composition and structure collected during wildfire incidents between 2005 and 2020, and remeasured these locations to establish a 20-year wildfire chronosequence. We used the original and remeasurement data to investigate (1) how forest structure before and after wildfire compares to the historic natural range of variability, (2) how immediate fire effects and environmental characteristics influence patterns of change in forest structure and biomass over time after wildfire, and (3) how fire changes forest C vulnerability to emission in future wildfires.

Methods

Study area

Our study area was located in mixed conifer and mixed conifer-hardwood forests in the Sierra Nevada and Klamath Mountain ecoregions of California, USA (Fig. 1a). Common tree species included *Pinus jeffreyi* Greville and Balfour (Jeffrey pine), *Pinus ponderosa* Douglas ex Lawson and C. Lawson (ponderosa pine), *Pinus lambertiana* Douglas (sugar pine), *Pseudotsuga menziesii* var. *menziesii* (Mirbel) Franco (Douglas-fir), *Abies concolor* (Gordon & Glendinning) Hildebrand (white fir), *Calocedrus decurrens* (Torrey) Florin (incense cedar), *Sequoiadendron giganteum* (Lindley) J. Bucholz (giant sequoia), and *Quercus kelloggii* Newberry (California black oak). Mixed-conifer forests were historically subject to frequent, low to moderate severity fires and have experienced overstory densification and uncharacteristic fuel accumulation over the previous century because of fire suppression and criminalization of cultural burning (Steel et al. 2015).

Study design

This study leveraged pre-existing plot locations and measurements collected between 2005 and 2020 during active wildfire incidents by the USDA Forest Service Fire Behavior Assessment Team (FBAT; Table 1). To assess long-term changes in forest vegetation and fuels since plot establishment, we remeasured all accessible FBAT plots ($n = 111$) in 2021–2025 (Fig. 2; Table 1). The remeasurement established a 20-year chronosequence experiment (i.e., a space-for-time substitution) to investigate changes in forest structure, composition, and fuels after wildfire. To our knowledge, no plots had been

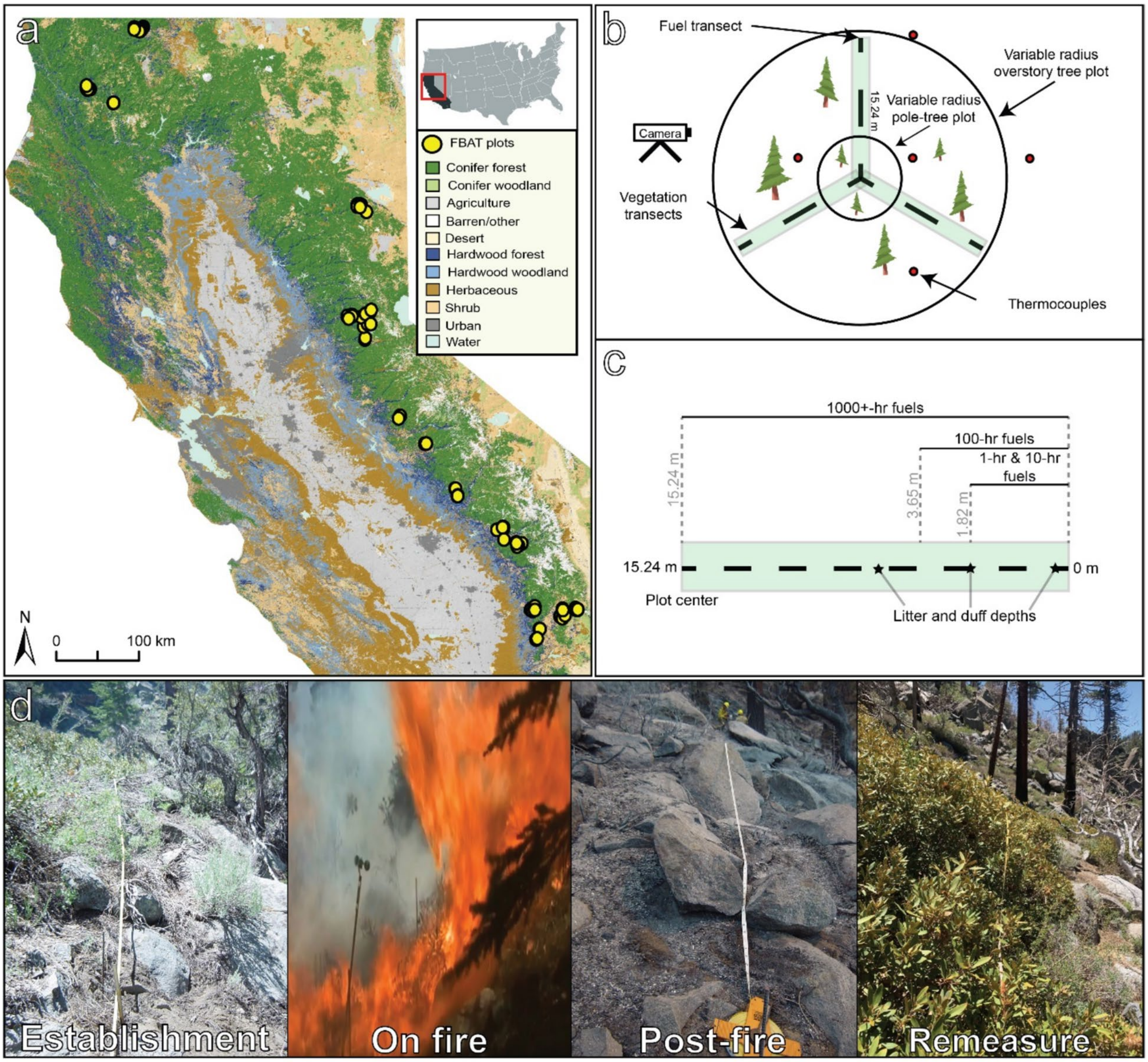

Fig. 1 Locations **a** of plots measured for this study, overlain on vegetation categories sourced from the California Department of Forestry and Fire Protection (2023). **b** Diagram of the measurements taken at each plot. **c** Diagram showing measurement locations along each of three replicate fuel transects within plot. **d** Pre-fire, during-fire, post-fire, and remeasurement photographs from the 2008 Clover fire, California, USA. Photo credit: Fire Behavior Assessment Team

burned within 20 years prior to establishment, and most had no recorded spatial history of wildfire since record keeping began (e.g., early 1900 s to present).

Plot establishment and remeasurement

FBAT established monitoring plots on active wildfire incidents across the Sierra Nevada and Klamath Mountain ecoregions, with plot locations chosen to be visually similar to the surrounding forest, in locations estimated to burn within days of plot establishment, and considering personnel safety. The FBAT established plots and measured forest composition, structure, and fuels typically 1–3 days prior to wildfire, installed instrumentation to collect active-fire weather and fire behavior characteristics (including video imagery; Fig. 1b; Reiner et al. 2021), and remeasured plots within 10 days after fire. The FBAT protocols were designed to balance the dual needs of precise data collection and safety in advance of approaching wildfire. Plots were monumented with rebar at plot center and at the origin of each of three

Table 1 Plot descriptions.The Fire Behavior Assessment Team (FBAT) plots remeasured in 2021–2025 in California, USA. Dominant overstory species include the two tree species with the greatest proportional live basal area at the time of remeasurement

Wildfire	Year	Burned	Control	Ecoregion	Elevation (m)	Dominant overstory species (basal area %)
Crag	2005	6	0	Sierra Nevada	2640–2656	*P. jeffreyi* (0.46)–*A. concolor* (0.30)
Ralston	2006	7	0	Sierra Nevada	922–1301	*Q. kelloggii* (0.28)–*P. ponderosa* (0.28)
Somes	2006	7	1	Klamath	419–1634	*P. menziesii* (0.92)–*N. densiflorus* (0.03)
Antelope	2007	3	1	Sierra Nevada	1707–1734	*P. ponderosa* (0.57)–*P. jeffreyi* (0.34)
Clover	2008	6	0	Sierra Nevada	2474–2525	*P. jeffreyi* (0.63)–*A. concolor* (0.28)
Lion	2011	6	0	Sierra Nevada	2048–2167	*P. ponderosa* (0.70)–*A. concolor* (0.29)
Beaver	2013	5	0	Klamath	1064–1441	*P. menziesii* (0.73)–*C. decurrens* (0.09)
Rim	2013	9	0	Sierra Nevada	1576–1875	*P. lambertiana* (0.42)–*P. ponderosa* (0.29)
King	2014	3	6	Sierra Nevada	1282–1989	*A. concolor* (0.33)–*C. decurrens* (0.33)
Rough	2015	12	4	Sierra Nevada	1221–2485	*A. concolor* (0.35)–*S. giganteum* (0.22)
Willow	2015	1	2	Sierra Nevada	1340–1594	*A. concolor* (0.34)–*P. jeffreyi* (0.22)
Cedar	2016	3	4	Sierra Nevada	1776–2132	*A. concolor* (0.35)–*C. decurrens* (0.30)
Pier	2017	5	0	Sierra Nevada	1486–1856	*C. decurrens* (0.38)–*A. concolor* (0.22)
Schaeffer	2017	1	9	Sierra Nevada	2312–2641	*P. jeffreyi* (0.38)–*P. ponderosa* (0.34)
Walker	2019	3	2	Sierra Nevada	1682–1724	*P. ponderosa* (0.59)–*P. jeffreyi* (0.25)
Red Salmon	2020	4	1	Klamath	642–712	*P. menziesii* (0.38)–*P. sabiniana* (0.25)
Total	–	81	30	–	419–2656	–

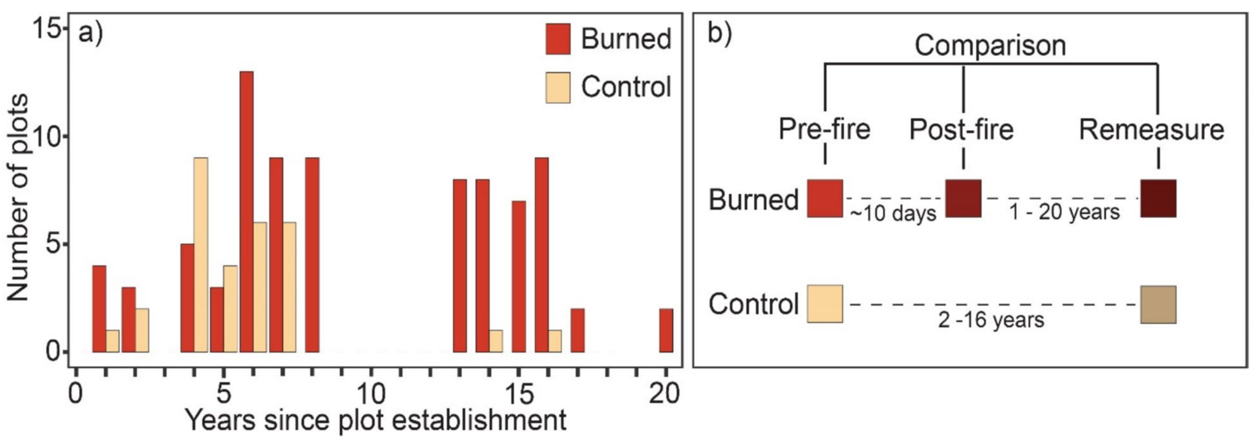

Fig. 2 **a** Distribution of Fire Behavior Assessment Team (FBAT) plots across number of years after fire for the chronosequence **b** of pre- and post-fire measurements (2005–2020) to remeasurement (2021–2025) events in California, USA

transects used for inventorying surface and ground fuels (hereafter, *fuels transects*; Fig. 1c). All plots were georeferenced during establishment to facilitate accurate relocation after the fire. Pre- and post-fire photographs were taken along each fuel transect. Unless otherwise noted, our 2021–2025 remeasurement methods followed the original FBAT methods used during plot establishment (Fire Behavior Assessment Team, 2022). Detailed protocols for the FBAT are available online (https://www.frames.gov/fbat/home). During our 2021–2025 remeasurements, we used plot coordinates and photographs to identify the vicinity of the original plots and searched for monumented rebar. Upon locating the rebar, we placed remeasurement transects along the same azimuths as the pre-fire transects. If rebar was not located, we placed our remeasurement plot at the closest location to the original coordinates, often guided by photos. Six plots had been logged after the fire, therefore we placed surrogate remeasurement plots in unlogged forest within 50 m of the original plot.

Some plots did not burn after their initial establishment ($n=30$) because the fire stopped before it reached the plot, and these were included as unburned reference stands (hereafter, *controls*) and remeasured using the same methods as burned plots. Burned plots ($n=81$) were those that had burned shortly after plot establishment and had been measured for post-fire characteristics by FBAT (hereafter, *burned*). We use 'pre-fire' to collectively refer to measurements taken from both burned and control plots at plot establishment, as the pre-fire measurements represent the unburned condition, regardless of whether the plots did or did not burn during the wildfire. The plots used for our present study spanned 419–2656 m of elevation across the Sierra Nevada and Klamath Mountain ecoregions and were broadly characteristic of forests with low–moderate severity fire regimes (Fig. S1). Though fire behavior and mode of fire spread (e.g., heading, backing) data exist for a portion of our plots, we did not analyze them in this study as it would have resulted in a sample size insufficient for analysis.

Tree measurements

We used a Spiegel Relaskop (Silvanus Inc.; Salzburg, Austria) to select trees for measurement in variable radius plots, with a Relaskop basal area factor that varied with the stem density of each plot. In general, we chose a basal area factor so that approximately 5–10 pole-sized trees (2.5–15.0 cm diameter at breast height; hereafter DBH) and 5–10 overstory trees (>15.0 cm DBH) were measured within each plot. The same basal area factor was maintained for plots in the same stand and during remeasurements. We identified the species and remeasured DBH, height, height to live crown, and health-related conditions (e.g., insect galleries or fire scars) for each tree. For all standing dead trees (hereafter 'snags'), we identified their decay classification (sensu Lutz et al. 2021), and visually estimated the top diameter of the stem to the nearest centimeter to aid mass estimations in cases of broken tops. We analyzed pole and overstory tree data together unless otherwise noted.

Surface and ground fuel measurements

In each plot, we placed three 15.24 m transects originating distal to the plot center (Fig. 1b) oriented at random azimuths in early years of FBAT plot installations and at 0°, 120°, and 240° azimuths in later years. Each transect was used for measuring downed woody fuels (hereafter, Brown's transects; Brown 1974) with the planar intercept method, and as the centerline of a belt transect to measure surface vegetation (Fire Behavior Assessment Team, 2022). Litter and duff layer depths at three locations (0, 1.8, and 4.8 m) were also measured on each transect. We measured tree seedlings, shrubs, grass, and forbs along each of the three 1.0 m × 15.24 m belt transects (Fig. 1c) centered on each Brown's transect. We estimated live and dead cover (percent area) and mean height and classified the bulk density and morphology for each species using the shrub and grass photoseries in Burgan and Rothermel (1984), with the modification of adapting shrub photoseries for seedlings and grass photoseries for forbs (Fire Behavior Assessment Team, 2022). Because phenology and plant identification skills varied among field crews and years, we did not analyze or report on the diversity of shrubs, grasses, or forbs.

We tallied 1–1000+h time lag fuels on each of the three 15.24 m Brown's transects (Brown 1974; Fig. 1c) as follows: intersections by 1 h (≤0.6 cm diameter) and 10 h (>0.6–2.54 cm diameter) fuels were tallied from 0 to 1.82 m along the transect, those of 100 h fuels (>2.54–7.6 cm diameter) were tallied from 0 to 3.65 m, and those of 1000+h fuels (>7.6 cm diameter) were tallied along the full transect. We grouped 1–100 h fuels (hereafter 'fine woody fuels') before analyzing changes and separately analyzed 1000+h fuels (hereafter 'coarse woody fuels').

Biomass calculations

We estimated the aboveground bole and foliage biomass of living trees following the allometric equations of Chojnacky et al. (2013) and Jenkins et al. (2003; Table S1:S2). Because *S. giganteum* tends to have large basal swells and we did not have permits to install guide nails to accurately measure DBH on large trees (>200 cm DBH), we do not analyze or report on live tree biomass or total ecosystem biomass for plots ($n=6$) with *S. giganteum* > 200 cm DBH (see Supplemental Information I for details on excluded plots). We estimated snag mass using species-specific equations (Harmon et al. 2008; Cousins et al. 2015; Table S3). We modeled snags of decay class ≥ 3 as conic frustums and used the volume to estimate snag biomass following the species and decay-specific values of Harmon et al. (2008). For tree seedlings, shrubs, grasses, and forbs, we used bulk density, average cover, and height to estimate biomass and then averaged biomass across the three transects (Burgan and Rothermel 1984). We calculated mass of fine woody fuels, coarse woody fuels, litter, and duff following Van Wagtendonk et al. (1998). Twelve plots were missing one or more fuel measurements from the pre-fire plot measurement events; these plots were excluded from analyses requiring complete data (see Supplemental Information I for details). To align with standard wildland fire terminology, we use the terms *fuel load* and *fuel loading* interchangeably with fuel mass, as a component of total forest biomass, all being measurements of mass per unit area. Our study focused on changes in total aboveground forest biomass, which we considered inclusive of the tree through duff layers.

Because consumption during fire varies among fuel classes (e.g., tree foliage versus boles versus litter; Miesel et al. 2018; Birch et al. 2023), for each fuel class we assessed its proportional contribution to total loading for all fuels that are vulnerable to consumption during wildfire (hereafter, 'potential fuel' with acknowledgment that fuel moisture content at the time of fire influences fuel availability as traditionally defined). Potential fuels include tree foliage, snags, seedlings, shrubs, grasses, forbs, fine and coarse woody fuels, litter, and duff. We included snags as potential fuels because they can be consumed by fires even under low burn severities (Becker and Lutz 2023) and during combustion may act as sources for embers, thereby contributing to greater fire energies and fire spread (Page et al. 2013; Birch et al. 2023). In contrast, biomass in each live tree bole is rarely consumed during the fire that causes a tree's mortality due to high live tissue moisture content and the presence of protective bark. For all estimations of C stocks or potential emissions, we used the approximation of 50.1% of woody biomass as C mass (Martin et al. 2018). We estimated pre-fire fuel moistures for fine and coarse woody fuels using spatially interpolated hourly weather data from remote automated weather stations and the FireFamilyPlus 5.0 program (Bradshaw and McCormick 2000; Régnière et al. 2018; sensu Birch et al. 2023).

Burn severity assessment

To relate changes in forest vegetation and fuel characteristics to initial fire effects, we retrieved the relativized delta normalized burn ratio (RdNBR) from the Monitoring Trends in Burn Severity database (Eidenshink et al. 2007). The RdNBR is a widely used relativized metric of the change in reflectance between LANDSAT image pairs taken before and after the fire, assessed at 30 × 30 m pixel scales (Miller and Thode 2007). The RdNBR is most sensitive to changes in overstory foliage reflectance (e.g., scorching or torching) and may not directly assess spatially heterogeneous fire effects or burn severity in strata beneath the overstory and at scales < 30 × 30 m (Miesel et al. 2018; Birch et al. 2025). We use continuous versions of the RdNBR rather than categorical burn severity (e.g., 'Low' or 'High') as our previous work found poor correspondence between fire effects and categorical burn severity (Birch et al. 2023). For most plots in this study, fire effects as measured by RdNBR were characteristic of low to moderate burn severity, whereas a few ($n = 12$) represented high-severity fire (Fig. S1; Monitoring Trends in Burn Severity 2023).

Characterizing topography and water limitations before and after fire

To characterize how overstory mortality and fuel accumulation related to drought stress after fire, we retrieved interpolated monthly weather (temperature, precipitation) from 1901 to 2021 using ClimateNA 7.31 (Wang et al. 2016) and used mean temperature values, plot latitude, and precipitation to calculate the Standardized Precipitation-Evapotranspiration Index (SPEI) with the SPEI 1.8.0 package (Beguería and Vicente-Serrano 2023). The SPEI is a standardized assessment of drought that is calculated using a climatic water balance and the accumulation of precipitation deficit or surplus over differing timescales (Vicente-Serrano et al. 2010). Negative (positive) values of SPEI are associated with water deficit (surplus). We calculated the monthly SPEI for each plot, using a 12-month window, to assess seasonal-scale drought conditions after burning (Fig. S2) when trees may be predisposed to delayed mortality. Because of temporal autocorrelation, we assess the mean SPEI only in the year after the fire.

To estimate the mean potential solar radiation at a given location, we calculated the McCune Heat Load for each plot using spatialEco 1.3.7 (Evans and Ram 2015) for each plot. The McCune Heat Load is an index from 0 to 1, where higher values indicate greater potential cumulative solar energy deposition, with solar radiation varying with slope, aspect, season, and latitude. We estimated a one-step topographic wetness index with a multiple-flow-direction algorithm in SAGA 7.9.1 (Conrad et al. 2015). We calculated each plot's slope, aspect, and elevation using a USGS 30 × 30 m digital elevation model (United States Geological Survey, 2020) in ArcGIS 10.6.1 (ESRI, Redlands, CA).

Comparing post-fire forest structure to the natural range of variability

To assess if forest structure after fire was more similar to the natural range of variability (NRV) than before fire, we compared forest structure at the pre-fire and remeasurement events to historical forest structure as determined from the Wieslander Vegetation Type Mapping dataset (VTM; Kelly et al. 2005, 2008). The VTM is representative of forest structure and composition in the 1920–1930s, shortly after effective widespread fire suppression began and many decades after genocide and criminalization of fire use largely ended indigenous burning. The VTM included tally counts, by tree species, and DBH size classes (Kelly et al. 2005, 2008), which we scaled to trees per hectare for comparison with our datasets. We retrieved and filtered observations of historical forest composition data from the VTM dataset using the LANDFIRE Biophysical Settings (LANDFIRE 2020) vegetation types, to include only those VTM plots in the same vegetation type, and with the same tree species, as our plots (Table S4). For comparison with the VTM data, we filtered our data to only include trees ≥ 10 cm, excluding most pole-sized trees, because these were not measured in the original VTM datasets.

Statistical analyses

To assess how fire effects and environmental factors influenced long-term changes in forest and fuel characteristics, we used a generalized additive model (GAM) approach to model both non-linear and linear relationships between variables. Our dependent variables included measures of the change in tree composition and structure, changes in fuel mass from the post-fire to remeasurement time-period, and changes in the proportional contribution of each fuel class to total ecosystem biomass among the pre-fire, post-fire, and remeasurement sampling events. We conducted all analyses in R 4.2.2 (R Core Team 2023) using the graphical user interface RStudio 1.3.1093 (R Studio Team 2023). We generated graphs using the ggplot2 3.3.3, ggpubr 0.4.0, and plotmo 3.6.2 R packages (Wickham 2016; Milborrow 2022; Kassambara 2023).

Our environmental explanatory variables included time since plot establishment, measures of site aridity and climate (elevation, McCune Heat Load, and topographic wetness), drought (post-fire SPEI), fire effects (percent canopy scorched and torched obtained during post-fire measurements [hereafter percent canopy affected], and RdNBR value), and total fire energy release (estimated from the total consumption of all fuels and a heat of combustion modified by fuel moisture; Wagner, 1972; Johnson 1996) as an empirical measure of fire behavior. Fire energy is a key variable in fireline intensity and provides an empirical measure of fire behavior (Table 2).

For each analysis, we used the mgcv 1.8–40 R package (Wood 2010, 2023), with GAM smoothing parameters selected by restricted maximum likelihood and constructed models for tree and fuel changes. We used the 'gam.check' function to assess smoothing parameter fits and manually adjusted smoothing parameters as needed. Due to sample size limitations, we restricted our explanatory variables to a maximum of four per model, to allow sufficient degrees of freedom for basis functions to fit non-linear patterns in the data. We used a forward model selection with all combinations of explanatory variables and selected our final model as that with the lowest Akaike information criterion.

We assessed compositional change in the live tree layer by calculating the abundance-based Bray–Curtis dissimilarity using the species-specific basal area between the pre-fire and remeasurement periods for each plot. Bray–Curtis dissimilarity does not provide directional information on change (e.g., pine to fir conversion) but rather indicates when communities are increasingly dissimilar (higher values). Two forests with completely (un-)similar structure would have a '0' ('1') value. Because the Bray–Curtis dissimilarity was bounded between 0 and 1, we used the 'betar' family of GAMs, with the modification that we adjusted 0 and 1 values by 0.0001 to exclude '0' and '1' values. To assess changes in fuel loadings between post-fire and remeasurement events, we grouped fuels measurements into broader categories based on their proximity in the forest, shared originating processes governing their accumulation, and expected similarity in influencing fire behavior (e.g., seedlings and shrubs, grasses and forbs, fine woody, coarse woody, litter, and duff). When assessing change in fuel mass between the pre-fire and remeasurement time points, we used the absolute change because the relative change could not be calculated when a particular fuel class was absent pre-fire. The absolute change in fuel mass was used as a dependent variable in separate GAM models for each type of fuel.

To assess how forest composition changed, we calculated species-specific basal area changes between pre-fire and remeasurement events. We calculated changes across only those plots in which a specific species occurred. Because of difficulty in differentiating *P. ponderosa* and *P. jeffreyi* in some plots where ranges overlap (Bradshaw 1941), we combined them into a 'yellow pine' grouping for all species-specific analyses. To compare

Table 2 List of a priori explanatory variables we tested to explain post-fire changes in forest composition, fuel biomass, and ecosystem carbon for plots in California, USA

Variable	Time-frame	Origin
Post-fire drought (SPEI)	Post-fire (1 year)	Calculated from interpolated climate data
McCune Heat Load	–	Calculated from DEM
Topographic wetness	–	Calculated from DEM
Elevation (m)	–	Calculated from DEM
Fire energy (MJ m^2)	During-fire	Calculated from fuel consumption
RdNBR	Post-fire (1 year)	Monitoring Trends in Burn Severity (2023)
Time since fire	Post-fire (1–20 years)	Fire Behavior Assessment Team (2022)
Canopy scorch (%)	Post-fire (1–10 days)	Fire Behavior Assessment Team (2022)

forest structure among the NRV, the pre-fire conditions (for control and burned plots), and the remeasured forest structure, we conducted a nonmetric multidimensional scaling (NMDS) ordination with 999 permutations for the number of tree stems, by size class, using the Mahalanobis distance measure using the vegan 2.6–4 R package (Oksanen et al. 2023). To understand what influenced the distribution of points in ordination space, we fit vectors of forest structure to the ordination using 999 permutations. We did not assess immediate post-fire forest structure in the NMDS because overstory tree mortality may not be apparent over short pre- to immediate post-fire time periods such as represented in the FBAT datasets.

We used analysis of variance (ANOVA) and a conservative Tukey's honest significant difference test in base R to test for pairwise differences in the mean values of forest and fuel characteristics (as described above) between pre-fire, post-fire and remeasurement conditions. For each ANOVA, we tested assumptions of normality using a Shapiro–Wilk test and homoscedasticity using a Bartlett test in base R (R Core Team 2023). Plots were assumed to be independent as they were typically separated on the landscape at scales ≥ 200 m.

To estimate the range of potential C emissions if plots were to reburn, we used the mean relative consumption percentage, by RdNBR burn severity class (Miller and Thode 2007), previously recorded in these plots (Birch et al. 2023). We used 51.3% snag consumption estimates of Becker and Lutz (2023), whose dataset co-occurs with four FBAT plots, has a larger sample size than our data, and is broadly representative of the fire behavior and low to moderate burn severity characteristic of our dataset. We multiplied each remeasurement type of fuel loading by the percent consumption, by severity class, and calculated the mean potential C emissions. To connect changes in potential fuels to burn severity we used linear regressions in base R to test (1) how pre-fire proportion of C in potential fuels related to RdNBR at the time of burning, and (2) how the proportion of C in potential fuels related between pre-fire and remeasurement sampling events.

Results

Changes in forest structure and comparison to the natural range of variability

Changes in tree-species basal area, as assessed by pairwise dissimilarity between pre-fire and remeasurement, were well-explained ($R^2 = 0.48$) by a GAM, with dissimilarity having no change with increasing time after fire (Fig. 3a; $P = 0.074$). Basal area dissimilarity had no clear relationship with fire energy (Fig. 3b; $P = 0.288$) and had greater dissimilarity from the pre-fire condition with increasing RdNBR values (Fig. 3c; $P < 0.001$). Basal area dissimilarity increased with wetter conditions in the year after fire (Fig. 3d; $P = 0.033$).

Because there were no patterns of change in basal area dissimilarity with time (Fig. 3a), we report mean changes in structure and composition between remeasurement and pre-fire conditions (median time since fire = 7 years; Table 3). Overstory tree density declined 50% in burned plots from 404 trees ha^{-1} pre-fire to 204 trees ha^{-1} at remeasurement whereas pole tree density was similar between pre-fire (723 poles ha^{-1}) and remeasurement (259 poles ha^{-1}; Table 3). Tree-layer height to live crown increased by 4.6 ± 0.6 m in the immediate post-fire environment, and this increase was largely retained at the time of plot remeasurement with a mean difference of 2.5 ± 0.7 m, relative to pre-fire (Table 3). Pre-fire and remeasurement trees per hectare by size class were similar to overstory Sierra mixed-conifer forests in the 1930 s and 1940 s (Fig. S3) for both burned and control plots, though NRV plots were more correlated with greater density of large-diameter stems (> 58 cm DBH) than plots from our modern dataset.

Live overstory biomass in burned plots declined between pre-fire and remeasurement by a mean of 101.0 ± 0.4 Mg ha^{-1} (SE) (Table 4). Live overstory basal area declined by 20.8 ± 3.0 m^2 ha^{-1} in burned plots and had no change in controls (Fig. S4), relative to pre-fire. The change in burned plot basal area at remeasurement was primarily caused by mortality of yellow pine species (8 ± 19% SE loss), *A. concolor* (15 ± 14% loss), *C. decurrens* (64 ± 10%), *Q. kelloggii* (77 ± 8% loss), and *P. lambertiana* (76 ± 12% loss) and ingrowth of *P. menziesii* (14 ± 125% gain; Fig. S4). Relative to the pre-fire measurements, snag mass increased by 281 ± 46% in the immediate post-fire environment and remained elevated at the time of remeasurement (249 ± 24%; Table 4). The GAM explaining the change in snag mass between post-fire and remeasurement events performed poorly ($R^2 = 0.21$), with no pattern with time since fire (Fig. 3e; $P = 0.925$) or fire energy (Fig. 3f; $P = 0.797$), but snag mass was lower with increasing RdNBR (Fig. 3g; $P = 0.027$), and greater with drier conditions in the year after fire (Fig. 3h; $P = 0.005$). Tree mortality and the subsequent addition of new snags between pre-fire and remeasurement increased the quadratic mean diameter of snags by 14.1 ± 4.3 cm, and the overall number of snags ha^{-1} (Table 3). The overwhelming majority of snags were of decay class 1 (mostly sound) at pre-fire (87.1%), post-fire (99.0%), and remeasurement (82.6%, Table S5).

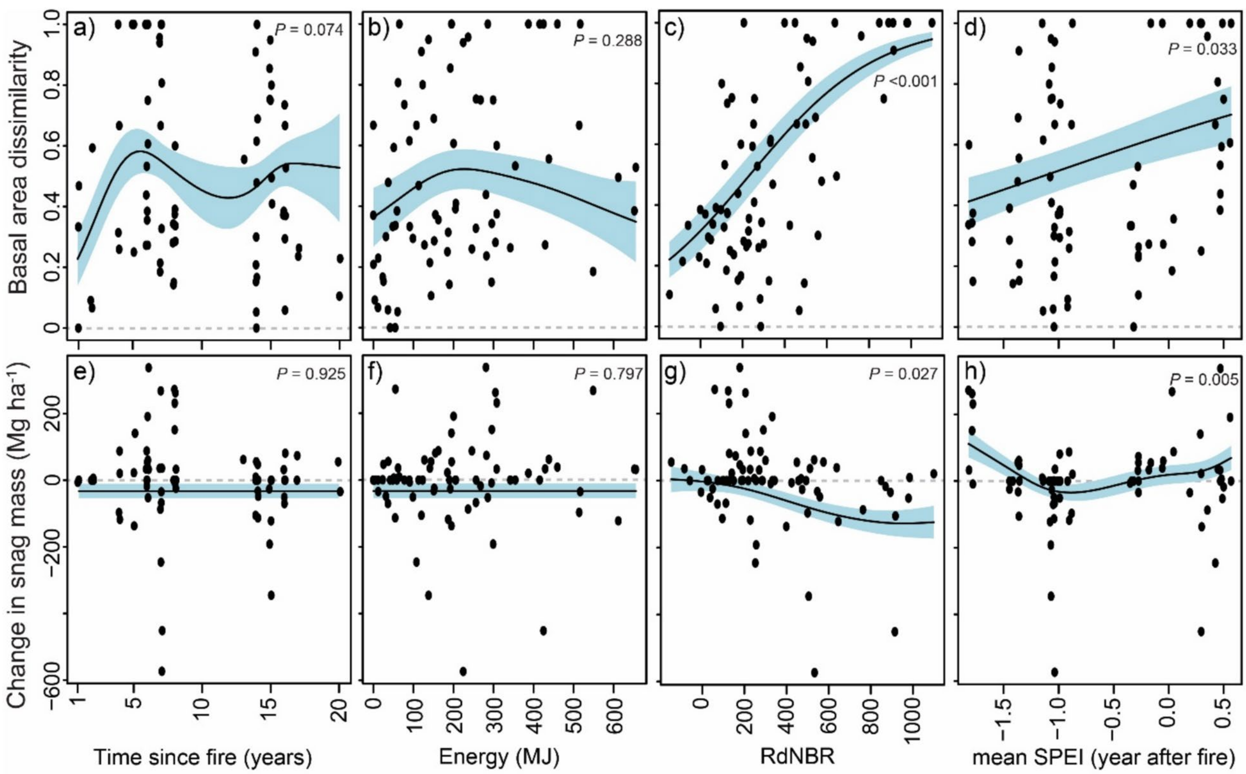

Fig. 3 Partial-effects plots with 95% confidence intervals (blue-shading) for pairwise Bray–Curtis dissimilarity (**a**–**d**) and change in standing dead tree (snag) loadings (**e**–**h**, Mg ha^{-1}) in California, USA, for **a**, **e** time since fire (y), **b**, **f** fire energy (MJ), **c**, **g** relativized delta normalized burn ratio (RdNBR), and **d**, **h** drought in the year after fire (SPEI). Higher (lower) Bray–Curtis dissimilarity indicate greater (lower) departures in species-specific basal area at remeasurement, relative to pre-fire

Table 3 Pre-fire, post-fire, and remeasurement forest structural characteristics

	Burned			Control	
Variable	Pre-fire	Post-fire	Remeasure	Pre-fire	Remeasure
Overstory trees per hectare	404 ± 53a	232 ± 32b	204 ± 29b	215 ± 35a	195 ± 35a
Pole trees per hectare	723 ± 381a	548 ± 386a	259 ± 84a	166 ± 61a	113 ± 50a
Snags per hectare	39 ± 9a	163 ± 42b	84 ± 1a	60 ± 23a	63 ± 18a
Overstory QMD (cm)	46.2 ± 2.4a	44.3 ± 3.4a	46.8 ± 3.2a	46.9 ± 4.0a	50.3 ± 4.7a
Snag QMD (cm)	21.6 ± 3.6a	31.0 ± 3.0ab	35.8 ± 4.2b	34.0 ± 7.6a	36.3 ± 6.0a
Height to live crown (m)	6.3 ± 0.4a	11.2 ± 0.6b	8.7 ± 0.6c	6.1 ± 0.6a	6.7 ± 0.6a
Tree height (m)	20.0 ± 0.9a	18.3 ± 1.3a	20.5 ± 1.3a	18.9 ± 1.5a	22.6 ± 2.7a
Snag height (m)	8.8 ± 1.6a	10.5 ± 1.2a	10.9 ± 1.4a	7.0 ± 1.6a	9.5 ± 1.8a

Mean ± 1 SE forest structural characteristics for plots in California, USA. Different letters indicate significant differences ($P < 0.05$) between mean values at differing sampling dates

QMD quadratic mean diameter

Changes in surface and ground fuels and associated factors

Changes in seedling and shrub biomass between post-fire and remeasurement events were negligible (Table 4) and explained little of the variation in our GAM model ($R^2 = 0.17$). There was no pattern with time since fire ($P = 0.467$; Fig. S5a), and no change with fire energy ($P = 0.610$; Fig. S5b), but seedling and shrub biomass were greater with RdNBR values > 400 ($P = 0.012$; Fig. S5c), and had no relationship with percent canopy scorched and torched ($P = 0.980$; Fig. S5d). Changes in forb and grass biomass between post-fire and remeasurement events

Table 4 Pre-fire, post-fire, and remeasurement fuel biomass (Mg ha^{-1}) and proportional contributions (%) to potential fuels

	Burned (Mg ha^{-1})			Control (Mg ha^{-1})	
Variable	**Pre-fire**	**Post-fire**	**Remeasure**	**Pre-fire**	**Remeasure**
Tree-layer*	294.0 ± 25.5a	231.9 ± 25.5a	192.9 ± 21.3b	250.0 ± 42.7a	237.3 ± 32.4a
Snags	27.8 ± 6.8a	78.2 ± 14.2b	69.3 ± 11.5b	39.2 ± 13.4a	67.9 ± 19.3a
Seedling	3.7 ± 2.8a	3.6 ± 2.8a	1.5 ± 0.5a	0.03 ± 0.02a	1.2 ± 0.6b
Shrub	4.8 ± 2.1a	0.6 ± 0.3b	2.7 ± 0.6ab	6.0 ± 2.6a	11.0 ± 4.5a
Grass	0.0 ± 0.0ab	0.0 ± 0.0a	0.1 ± 0.0b	0.0 ± 0.0a	0.1 ± 0.1a
Forb	0.0 ± 0.0a	0.0 ± 0.0a	0.3 ± 0.2a	0.0 ± 0.0a	0.0 ± 0.2a
1000+-h	35.0 ± 7.2a	5.7 ± 1.4b	36.4 ± 7.5a	15.4 ± 3.7a	33.9 ± 6.4b
100-h	3.9 ± 0.4a	0.5 ± 0.1b	4.0 ± 0.5a	4.7 ± 0.8a	2.7 ± 0.3b
10-h	2.6 ± 0.2a	0.5 ± 0.1b	5.1 ± 0.6c	2.5 ± 0.2a	4.8 ± 0.5b
1-h	0.7 ± 0.1a	0.1 ± 0.0b	0.8 ± 0.0a	0.9 ± 0.1a	0.8 ± 0.1a
Litter	19.5 ± 2.7a	2.6 ± 0.4b	12.9 ± 1.2c	17.7 ± 2.1a	19.8 ± 2.6a
Duff	41.5 ± 3.8a	6.7 ± 1.2b	28.1 ± 2.1c	52.1 ± 9.0a	51.2 ± 6.1a
Total fuels	155.6 ± 13.4	106.8 ± 14.2b	172.4 ± 14.6a	151.0 ± 18.1a	207.0 ± 22.0a
Total mass*	433.9 ± 28.5a	300.6 ± 27.3b	354.8 ± 24.1a	380.1 ± 49.2a	431.2 ± 46.5a
Proportional contribution to potential fuels (%)					
Foliage*	16.3 ± 1.7a	22.8 ± 3.2b	11.0 ± 1.4a	10.8 ± 1.6a	7.4 ± 1.1a
Snags	12.0 ± 2.1a	46.9 ± 4.8b	27.6 ± 3.4c	19.7 ± 5.1a	21.6 ± 4.7a
Seedling	1.4 ± 0.8a	2.0 ± 1.2a	1.3 ± 0.3a	0.0 ± 0.0a	0.6 ± 0.3b
Shrub	4.2 ± 1.3a	1.6 ± 0.7a	1.8 ± 0.3b	5.1 ± 2.6a	6.0 ± 2.2a
Grass	0.0 ± 0.0a	0.0 ± 0.0a	0.2 ± 0.0a	0.0 ± 0.0a	0.1 ± 0.1a
Forb	0.0 ± 0.0a	0.0 ± 0.0a	0.3 ± 0.2a	0.0 ± 0.0a	0.0 ± 0.0a
1000+ -h	16.5 ± 2.5a	6.9 ± 1.7b	17.0 ± 2.1a	13.0 ± 3.2a	19.8 ± 3.5a
100-h	3.4 ± 0.5a	1.6 ± 0.5b	3.2 ± 0.4a	4.3 ± 0.9a	1.4 ± 0.1b
10-h	2.7 ± 0.5a	1.6 ± 0.6a	4.0 ± 0.4b	2.0 ± 0.2a	3.3 ± 0.6b
1-h	0.6 ± 0.0a	0.3 ± 0.0b	0.7 ± 0.0a	0.7 ± 0.0a	0.4 ± 0.0a
Litter	14.0 ± 1.3a	6.0 ± 1.1b	10.1 ± 0.8a	13.8 ± 1.4a	11.3 ± 1.7a
Duff	28.4 ± 2.2a	14.2 ± 2.4b	22.4 ± 1.9a	32.6 ± 4.0a	27.4 ± 3.2a

Mean ± 1 SE biomass for Fire Behavior Assessment Team plots in California, USA. Different letters indicate significant differences ($P < 0.05$) between sampling dates

(Table 4) were negligible and were poorly explained by the GAM model ($R^2 = 0.11$) with a slightly negative trend with increasing time since fire ($P = 0.004$; Fig. S5) and no significant patterns with other explanatory variables (Fig. S5e:h).

The mass of all fine woody fuels at remeasurement was similar to or exceeded pre-fire conditions (Table 4; median time since fire = 7 years). The changes in fine woody fuel biomass between post-fire and remeasurement were poorly explained by the GAM ($R^2 = 0.19$). Fine woody fuels increased slightly in the 7 years after fire ($P = 0.009$: Fig. 4a), had no change with fire energy ($P = 0.281$; Fig. 4b), were lower at RdNBR values > 600 ($P = 0.024$; Fig. 4c), and exhibited no relationship with drought in the year after fire ($P = 0.097$; Fig. 4d). At the median time of remeasurement (7 years), coarse woody fuel mass was similar to pre-fire levels (Table 4) and the change in coarse woody fuel mass between post-fire and remeasurement events was poorly explained by a GAM model ($R^2 = 0.09$). The change in coarse woody fuel mass had a marginally significant trend of increasing with time since fire ($P = 0.073$; Fig. 4e), no change with fire energy ($P = 0.485$; Fig. 4f), increased with higher RdNBR ($P = 0.023$; Fig. 4g), and showed no pattern with drought in the year after fire ($P = 0.882$; Fig. 4h).

At the median time of remeasurement (7 years), litter and duff mass were collectively lower than pre-fire (Table 4) and the rates of accumulation between post-fire and remeasurement were poorly explained by a GAM model ($R^2 = 0.24$). Combined litter and duff mass increased in the seven years after fire ($P = 0.001$; Fig. 4i), increased with fire energy ($P = 0.006$; Fig. 4j), and showed no patterns with RdNBR ($P = 0.460$; Fig. 4k) or drought in the year after fire ($P = 0.763$, Fig. 4l).

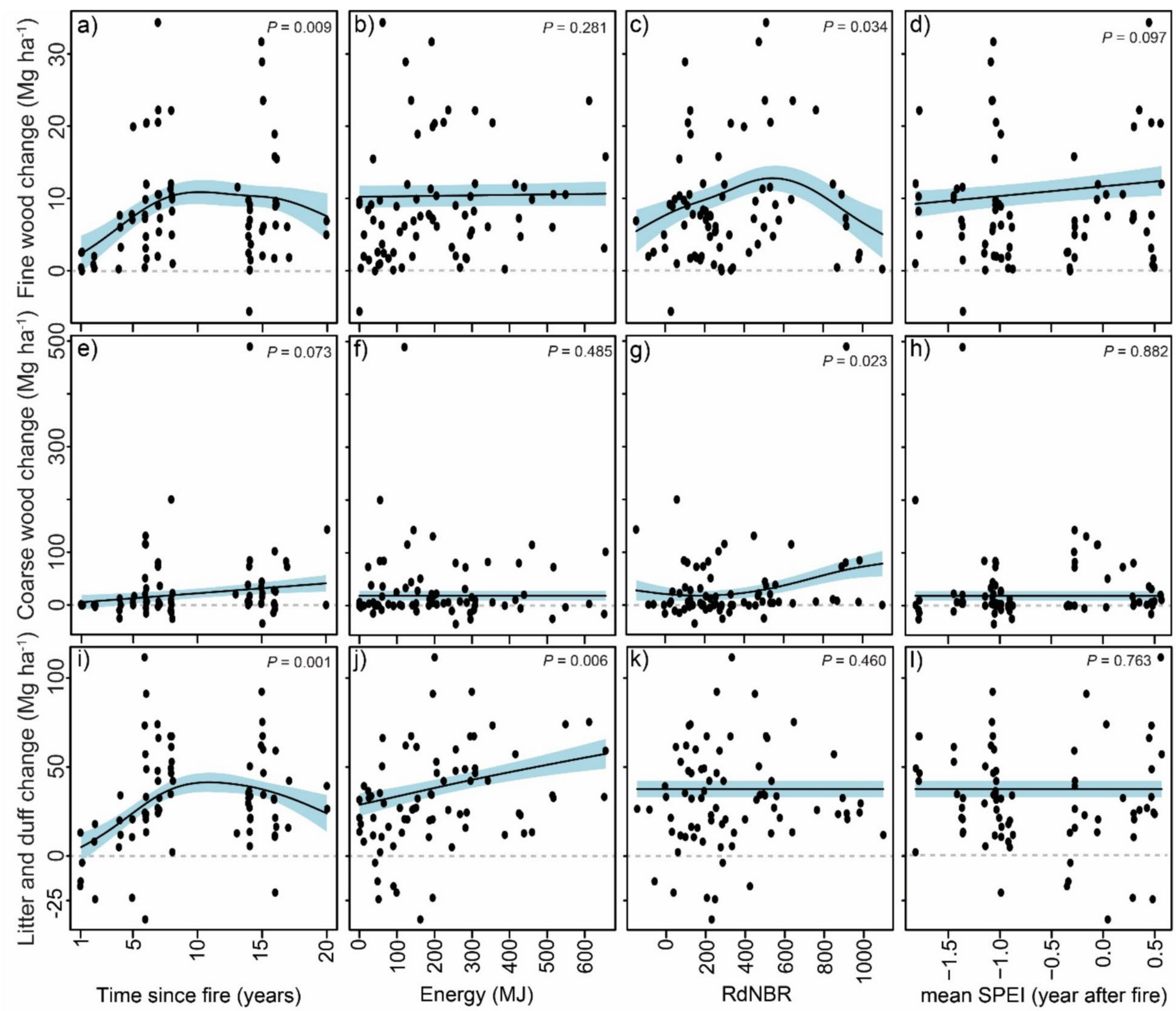

Fig. 4 Partial effects plots with 95% confidence intervals (blue-shading) for change in fine woody fuel (Mg ha^{-1}; **a**–**d**), coarse woody fuel (Mg ha^{-1}; **e**–**h**), and litter and duff fuel (Mg ha^{-1}; **i**–**l**) between post-fire and remeasurement in California, USA. **a**, **e**, **i** Time since fire, **b**, **f**, **j** fire energy (MJ). **c**, **g**, **k** Relativized delta normalized burn ratio (RdNBR). **d**, **h**, **l** Drought in the year after fire (SPEI). Values above (below) '0' on the y-axis indicate greater (lower) fuel mass at the time of remeasurement, to relative to pre-fire

Post-fire changes in the distribution of fuels and vulnerability of carbon to emission in future fire

At the median time of remeasurement (7 years), the fuel mass vulnerable to loss during fire (i.e., potential fuel load: tree foliage, snags, seedling, shrub, grass, forb, fine and coarse woody fuels, litter, and duff) had accumulated to values consistent with pre-fire conditions and the relative proportion of each fuel class out of total potential fuel load generally remained unchanged between pre-fire to remeasurement (Fig. 5; Table 4). Notably, snags increased from 12.0 ± 2.1% pre-fire to 27.6 ± 3.4% of potential fuel at remeasurement, the largest shift of any fuel class. At remeasurement, potential fuels in burned plots represented 52 ± 3% of aboveground ecosystem biomass, compared to 38 ± 2% pre-fire and 37 ± 3% post-fire (Fig. 5). The pre-fire proportion of ecosystem C existing as potential fuels was positively associated with RdNBR ($y = 471.11x + 136.00$, $R^2 = 0.12$, $P = 0.001$, Fig. S6). Forests with greater proportions of pre-fire C as potential fuels had increases in their proportions of ecosystem C as potential fuels at remeasurement ($R^2 = 0.24$, $P < 0.001$, Fig. 5c). Because these fuels are highly susceptible to consumption during fire, future reburns could produce mean C emissions ranging from 48.5 Mg ha^{-1} (unchanged to very low RdNBR burn severity), 55.5 Mg ha^{-1} (low severity), 61.1 Mg ha^{-1} (moderate), or 67.0 Mg ha^{-1} (high),

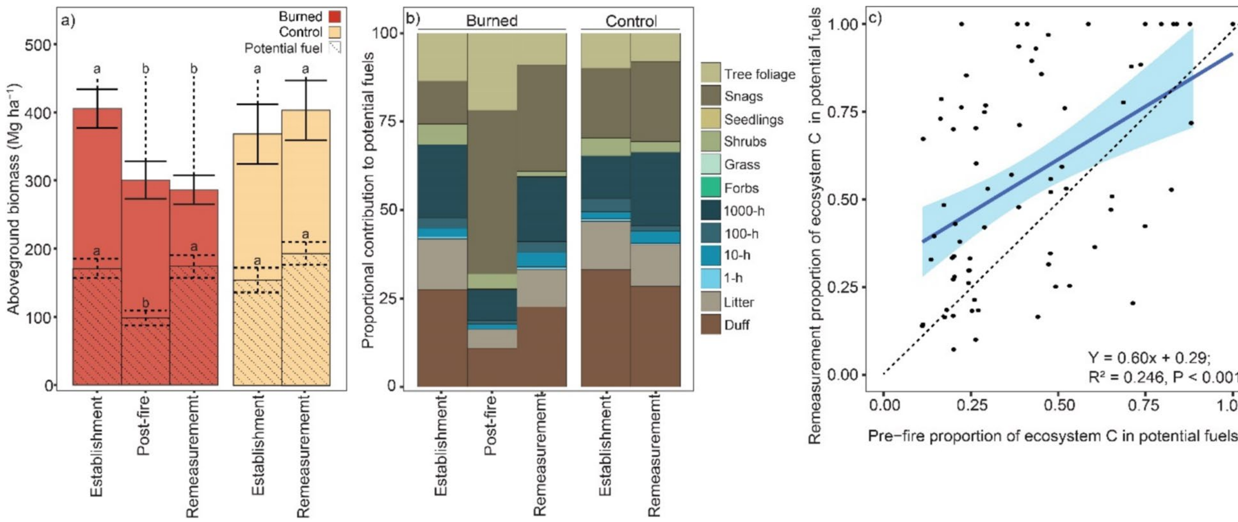

Fig. 5 Mean (± 1 SE) total aboveground biomass and potential fuel load vulnerable to consumption (**a**); relative contribution of each fuel class to total potential fuel load (**b**) at pre-fire, immediate post-fire, and remeasurement; and **c** the linear relationship with 95% confidence intervals (blue-shading) between the proportion of aboveground C in potential fuels pre-fire and at remeasurement in California, USA. Bars are grouped separately for burned and control plots, with different lowercase letters indicating significant differences between sampling periods

assuming similar fire behavior and consumption estimates as prior FBAT-recorded fires (Table S6).

Discussion

Post-fire forests are more similar to the natural range of variability

Our results indicate that reductions in forest densities due to the immediate effects of fire plus delayed mortality increased similarity to the historic natural range of variability (NRV). Fire shifted stand densities from a pre-fire high of 404 ± 53 trees ha^{-1} to 204 ± 29 trees ha^{-1} at remeasurement, a value comparable to USFS timber inventories in 1923 which recorded a mean of 128 trees ha^{-1} (Stephens et al. 2018). Though it is likely that pre- and post-fire forests in our dataset were deficient in large-diameter stems (e.g., > 92 cm DBH; Fig. S3) relative to the NRV. Whereas overstory stand densities were similar to the NRV, it is likely that fire-intolerant *Abies* spp. are present in much greater abundance in both the pre-fire and remeasurement conditions relative to the NRV (Steel et al. 2015).

A 2.5 ± 0.7 m increase in height to live crown persisted through the median remeasurement, and, together with survival of large trees and reduced stand density, may increase resistance to future wildfire mortality and facilitate low-intensity surface fire behavior during wildfires and prescribed fire treatments (Cruz et al. 2004; Zhang et al. 2019; Birch et al. 2026). As well, decreases in stand density can reduce competition for water (Vernon et al. 2018; Schmitt et al. 2020), thereby reducing stress and density-dependent mortality, which together can increase tree resilience to drought stress, pests, or pathogens (Birch et al. 2019; Germain and Lutz 2024).

Few identifiable drivers of snag loadings and the accumulation of fine and coarse woody fuels

High variability in fuel accumulation rates in our study limited our ability to identify generalizable drivers and thresholds of forest change after wildfire. The biomass (i.e., fuel loading) for most fuel classes equaled or exceeded pre-fire mass—likely because fire-killed and other snags deposited fine and coarse woody fuels in the decade after fire. On average, most fire-originated snags fragment or fall within 2–15 years after fire (Ritchie et al. 2013; Becker and Lutz 2023; Peterson et al. 2023), a timeframe consistent with the accumulation of surface and ground fuels in our study. However, the absence of any significant decline in snag density and mass over time since fire in this study suggests that many of the snags originating from wildfire may already have fragmented or fallen by the median time of our remeasurement (7 years) and were replaced by new snags produced from delayed tree mortality. Snag retention rates can drive post-fire fuel accumulation (Roccaforte et al. 2012), and we expect that other systems with slower snag decay rates, such as Canadian boreal mixedwoods (15–26 years for 50% retention; Angers et al. 2010), may have slower surface fuel accumulation commensurate with lower rates of snag fragmentation and deposition.

Delayed tree mortality leading to snag creation can result from indirect fire effects that manifest over time after a site is burned; for example, fire-induced necrosis of live tissues may induce stress that predisposes or prevents defense against bark beetle attack (Jenkins et al. 2013), pathogens (Maringer et al. 2016), or contribute to mechanical failure (Franklin et al. 1987; Shive et al. 2022). Compounding disturbances (e.g., drought and bark beetle disturbances between 2013 and 2015) likely contributed to delayed overstory mortality and elevated snag density (Butler and Dickinson 2010; Goulden and Bales 2019; Keen et al. 2022; Reed and Hood 2023).

Dense concentrations of snags can make wildfire behavior more difficult to manage due to safety concerns for firefighters as well as by contributing to elevated intensity and spotting (Page et al. 2013). Snags at remeasurement were largely non-rotten and of decay class 1 (82.6%) or 2 (12.7%) which are less likely to be fully consumed during a fire than are snags of advanced decay (Stockstad 1979; Becker and Lutz 2023; Table S5). Over time, snag decay contributes to coarse woody fuels—a type of fuel which is 62–91% more vulnerable to consumption than snags (Birch et al. 2023; their Table 4).

We expected that worsening drought (lower SPEI) in the year after fire would be associated with greater overstory mortality and therefore fuel loadings at remeasurement. However, the SPEI in the year after burn was frequently included in the best-performing models but had unclear directionality or marginal significance for changes in overstory basal area and fine and coarse woody fuels. Similarly, the topographic wetness index and McCune Heat Load, which are indirect measures of moisture availability, were absent from all top-performing models. Other researchers also have reported an unclear relationship between post-fire tree mortality and drought (Barker et al. 2022; Reed and Hood 2023), which can arise from physiological differences among and between tree species or an easing of competition for water in a fire-thinned overstory. Despite the unclear associations reported here and elsewhere, we broadly expect that aridity and drought stress will drive more severe fire effects owing to lower fuel moistures (Rao et al. 2022), and by inducing stress and contributing to cavitation during and after fire (Hood et al. 2018; Furniss et al. 2020).

Fire increases vulnerability of carbon stocks to consumption under future wildfire

The transition from live to dead biomass pools (i.e., live trees to snags) and accumulation of fine and coarse woody fuels indicates that the fires in our study increased forest C vulnerability to emission in future wildfires, by increasing the loadings of fuel classes most likely to be consumed. Work by Tortorelli et al. (2024) found that reburns that occur within 13 years after low to moderate severity fires, such as those in our dataset, are likely to have moderated impacts on the overstory because of altered forest structure from the first fire, and slow accumulation of fuels. Based on our study, the weakly positive trend between RdNBR and the pre-fire portion of ecosystem C contained in potential fuels (Fig. S6), as well as increases in the proportions of ecosystem C in potential fuels at remeasurement (Fig. 5c) together suggest that future reburns may be of slightly greater burn severity than past burns. However, high consumption of surface fuels and corresponding C emissions may not directly translate to loss of live overstory C stocks, as surface and ground fuel consumption are weakly linked to overstory mortality in California mixed-conifer forests ($R^2 = 0.34$; Birch et al. 2023)—particularly in cases where consumption occurs away from tree crowns, boles, and surface roots (Hood et al. 2018).

Despite elevated canopy base heights, reduced stem density, and unchanged overstory quadratic mean diameter, the C pools vulnerable to loss in fire had accumulated within a decade after fire to conditions similar to the pre-fire status. Notably, the 12% proportional increase in potential fuels, to 52% of aboveground ecosystem C, highlights the potential for large losses of stored C via high C emissions in future wildfires (Table S6). Our reported proportion of C vulnerable to future fire is similar to the upper range reported shortly after high severity wildfire in Australian sclerophyll forests (e.g., 20–60% aboveground C; Nolan et al. 2022), though our reported absolute and relative consumption rates are greater across coarse and fine woody fuels than those estimated in Australia (Nolan et al. 2022; Volkova et al. 2022). Given the uncertainty in estimating consumption from post-fire measurements alone, more co-located pre-fire and post-fire measurements in other systems are needed to identify how pre-fire fuel structure and fuel consumption relate to post-fire changes in C pools and their vulnerability to future fire.

Apart from contributing to further climate forcing of wildfire regimes (Liu et al. 2014; Abatzoglou et al. 2019), consumption of accumulated fuels may drive high-intensity wildfire behavior with a greater risk of high overstory mortality and stable state conversion (Serra-Diaz et al. 2018; Stephens et al. 2022) and result in large pulses of atmospheric particulate matter harmful to human health (Xu et al. 2024). As well, subsequent wildfires may compound existing fire injuries (e.g., partial girdling or fire scars; Shive et al. 2022) leading to mechanical failure, or—in combination with environmental stressors—reduce tree resistance to even low-intensity wildfire. Our assessments of post-fire changes in fuel accumulation and overstory structure are likely not applicable for forests that burn under wind-driven, high-intensity fires (e.g., Goforth and Minnich 2008) or forests in more marginal, water-limited habitat that may be more prone to stable state conversion outside of the NRV (Hill et al. 2023), neither of which are well-represented by our dataset.

The effects of wildfire on plots in this study were primarily low to moderate severity (Fig. S1), the type of fire which is often claimed as a hazardous fuel treatment for vegetation types that historically burned at frequent intervals. For example, the US Forest Service may claim acreage as hazardous fuel reduction in the Forest Activity Tracking System (United States Forest Service 2024) where it meets management objectives. Fuel reductions, snag densities, and C vulnerabilities in our dataset may thus be representative of the types of fire effects to be expected from wildfire managed for resource benefit or prescribed fire in long-unburned mixed-conifer forests with unmanaged fuels. Future fire managed for resource benefits in our study area will likely produce mean C emissions of 48.5–55.5 Mg ha^{-1} (Table S6); however, such estimates remain lower than estimated C emissions under high severities (e.g., > 67.0 Mg ha^{-1}). A previous analysis of this dataset showed that fuel consumption (and energy release) is mitigated in backing fires relative to heading fires (Birch et al. 2023); thus, fuel consumption can be influenced by fire management actions (e.g., through ignition operations) and, along with fuel treatments (especially prescribed fire), can help reduce undesirable fire effects.

Reducing fuels through greater use of managed wildfire or prescribed fire may iteratively reduce excessive fuel mass and prevent future high severity fires. For example, even under weather-driven fire behavior, burn severity may be moderated when wildfires burn through areas previously treated with prescribed fire (Brodie et al. 2024; Birch et al. 2026). Given the inadequate pace and scale of prescribed fire and thinning (North et al. 2021), greater use of managed wildfire in combination and in addition to repeated and gradual reintroduction of prescribed fire, coupled with mechanical treatments where feasible, are likely needed to avoid high-severity wildfire over large areas in California mixed-conifer forests (Hurteau et al. 2024). This may preempt positive feedback cycles where high-severity wildfire leads to abundant post-fire fuel deposition and therefore more high-severity wildfire (Coppoletta et al. 2016; Harris et al. 2021).

Conclusion

Our results support the expectation that fire under certain conditions can improve forest resilience to detrimental wildfire impacts in future fires by decreasing forest stand density and increasing height to live crown, despite mean consumption of 61.1 Mg ha^{-1} C. However, the increase in snag abundance and biomass, and accumulation in fine and coarse woody fuels returned potential fuel loadings to pre-fire levels within a decade. Thus, the carryover and accumulation of fuels raises concern about the potential for large C emission events in future wildfire. Achieving resilience in these and similar dry, fire-suppressed, and fuel-dense forest types may be achieved through management intervention such as low-intensity prescribed burns or managed low-intensity wildfires that produce only low-severity impacts on the canopy while incrementally reducing the loadings and accumulation rates of fuels available for future fires.

Abbreviations

DBH	Diameter at breast height
DEM	Digital elevation model
FBAT	Fire Behavior Assessment Team
GAM	Generalized additive model
RdNBR	Relativized delta normalized burn ratio
NMDS	Nonmetric multidimensional scaling
NRV	Natural range of variability
QMD	Quadratic mean diameter
SPEI	Standardized precipitation-evapotranspiration index
VTM	Wieslander vegetation type mapping

Supplementary Information

The online version contains supplementary material available at https://doi.org/10.1186/s42408-026-00510-7.

Supplementary Material 1. Table S1. Allometric equations used to estimate living tree biomass for species present in our study sites, California, USA. Where biomass is calculated as: ln(biomass(kg)) = $\beta_0 + \beta_1 \times$ ln(diameter at breast height [DBH], cm) (Chojnacky et al. 2013; Miles, 2009). Table S2. Component parameters we used to estimate biomass (kg) for the live foliage, bark, stem wood, and coarse roots for all pole and overstory trees. Biomass components are calculated as: biomass(kg) = exp($\beta_0 + \beta_1 \times$ ln(diameter at breast height, cm) (Jenkins et al. 2003). Table S3. Species-specific density conversion factors used to convert live biomass to estimated biomass of standing snags, by decay classification (Harmon et al. 2008). Table S4. The LANDFIRE Biophysical Setting (BPS) classification (LANDFIRE 2020) and the number (N) of Fire Behavior Assessment Team (FBAT) and Wieslander Vegetation Type Mapping dataset (Kelly et al. 2005, 2008) plots within each category in California, USA. Table S5. The proportion of decay classes (sensu Lutz et al. 2021) recorded for standing dead trees pre-fire, post-fire, and at remeasurement in California, USA. Table S6. Estimates of mean and maximum C emissions (Mg ha^{-1}) under differing RdNBR severity classes (Miller and Thode 2007) in California, USA. Percent consumption estimated using data from Birch et al. (2023, their Table 4) and Becker and Lutz (2023) and consumed fuels multiplied by 0.5 to estimate C consumed (Martin et al. 2018). Figure S1. Cumulative distribution of relative delta normalized burn ratio (RdNBR) values for all Fire Behavior Assessment (FBAT) plots 2005–2020 and for in all fires (> 400 ha) in the Sierra Nevada and Klamath Mountain ecoregions, California, USA (Miles and Goudey, 1997). Higher (lower) RdNBR values are associated with more (less) severe fire effects. All fire perimeters and RdNBR were sourced from the Monitoring Trends in Burn Severity (Monitoring Trends in Burn Severity 2023) program for the period 2005–2020. Figure S2. Standardized Precipitation-Evapotranspiration Index (SPEI) values averaged over the 12-month periods before (negative year values) and after (positive year values) the year of burn ('Year 0')in plots in California, USA. Values of SPEI < 0 (> 0) indicate drought (mesic) conditions Figure S3. Nonmetric multidimensional scaling (NMDS) ordination representing community dissimilarity in trees per hectare, by size class, between the pre-fire establishment plots, the burned and control plots at the time of remeasurement, and the historical Wieslander plots from the 1920 s – 1930 s (Kelly et al. 2005, 2008) which represent a condition more similar to but potentially still departed from the natural range of variability (NRV) in California mixed-conifer forests. Ellipses represent 95% confidence intervals for group centroids. Vectors indicate significant correlations ($P < 0.001$) between the size of trees and ordination space. Figure S4. Mean ± 1 SE change in basal area (%) by tree species, between pre-fire and remeasurement for burned and unburned control forests in California, USA. Yellow pine grouping include both *Pinus ponderosa* and *Pinus jeffreyii*, due to hybridization. Figure S5. Partial effects plots with 95% confidence intervals (blue-shading) for change in shrub and seedling fuels (Mg ha^{-1}; a-d) and grass and forb fuels (Mg ha^{-1}; e–h) between postfire and remeasurement in California, USA. (a, e,) Time since fire. (b, f) Fire energy (MJ). (c, g) Relative delta normalized burn ratio (RdNBR). (d, h) Percent canopy affected (%). Values above (below) '0' on the y-axis indicate greater (lower) fuel mass at the time of remeasurement, relative to relative to pre-fire. Figure S5. The positive, linear relationship with 95% confidence intervals (blue-shading) between the pre-fire proportion of aboveground ecosystem C in potential fuels and the relative delta normalized burn ratio (RdNBR) in California, USA

Acknowledgements

We appreciate the support of the many Fire Behavior Assessment Team members who contributed to generating the dataset. We thank the USFS Northern Research Station, Washington Office, and Pacific Southwest Region Fire and Aviation Management programs and the Joint Fire Science Program for logistical and financial support for the Fire Behavior Assessment Team since its establishment. We acknowledge that Native American peoples are the original stewards of the lands on which our sites are located, and we recognize past roles in suppressing cultural land management practices such as indigenous fire stewardship. We are appreciative for the R Project and the many developers who support the statistical and processing packages. We thank the U.S. Forest Service ranger districts for coordinating plot access.

Authors' contributions

JDB, MD, JM, and EK conceived the study. JDB, CE, and MD collected data. JDB analyzed data. All authors contributed to synthesis, writing, and editing.

Funding

Funding for this project was provided by the California Department of Forestry and Fire Protection (Grant number 8GG19804) as part of the California Climate Investments Program, with partial support from the Joint Fire Science Program (BLM-JFSP-2023–000217) and the McIntire-Stennis program (Projects MICL06033 and IDAZ-MS-0132).

Data availability

Data and code available upon reasonable request.

Declarations

Ethics approval and consent to participate

Not applicable.

Consent for publication

Not applicable.

Competing interests

The authors declare no competing interests.

Author details

[1]Department of Plant, Soil and Microbial Sciences, Michigan State University, East Lansing, Michigan 48823, USA. [2]Program in Ecology, Evolution and Behavior, Michigan State University, East Lansing, Michigan 48823, USA. [3]USDA Forest Service, Northern Research Station, Delaware, OH 43015, USA. [4]USDA Forest Service, Pacific Southwest Research Station, Redding, CA 96002, USA. [5]USDA Forest Service, PSW Region, Vallejo, CA 95370, USA. [6]Department of Forest, Rangeland and Fire Sciences, University of Idaho, Moscow, ID 83844, USA.

Received: 23 December 2024 Accepted: 5 May 2026
Published online: 01 June 2026

References

Abatzoglou, J. T., and A. P. Williams. 2016. Impact of anthropogenic climate change on wildfire across western US forests. *Proceedings of the National Academy of Sciences* 113:11770–11775. https://doi.org/10.1073/pnas.1607171113.

Abatzoglou, J. T., A. P. Williams, and R. Barbero. 2019. Global emergence of anthropogenic climate change in fire weather indices. *Geophysical Research Letters* 46:326–336. https://doi.org/10.1029/2018GL080959.

Angers, V. A., P. Drapeau, and Y. Bergeron. 2010. Snag degradation pathways of four North American boreal tree species. *Forest Ecology and Management* 259:246–256. https://doi.org/10.1016/j.foreco.2009.09.026.

Ayars, J., H. A. Kramer, and G. M. Jones. 2023. The 2020 to 2021 California megafires and their impacts on wildlife habitat. *Proceedings of the National Academy of Sciences* 120 : e2312909120. https://doi.org/10.1073/pnas.2312909120.

Barker, J. S., A. N. Gray, and J. S. Fried. 2022. The effects of crown scorch on post-fire delayed mortality are modified by drought exposure in California (USA). *Fire* 5 : 21.

Becker, K. M. L., and J. A. Lutz. 2023. Predicting snag fall in an old-growth forest after fire. *Fire Ecology* 19:71. https://doi.org/10.1186/s42408-023-00225-z.

Beguería, S., Vicente-Serrano, S.M., 2023. *SPEI: calculation of the standardized precipitation-evapotranspiration index* 1.8.0. https://CRAN.R-project.org/package=SPEI.

Birch, J. D., J. A. Lutz, S. W. Simard, R. Pelletier, G. H. LaRoi, and J. Karst. 2019. Density-dependent processes fluctuate over 50 years in an ecotone forest. *Oecologia* 191:909–918. https://doi.org/10.1007/s00442-019-04534-6.

Birch, J. D., M. B. Dickinson, A. Reiner, E. E. Knapp, S. N. Dailey, C. Ewell, J. A. Lutz, and J. R. Miesel. 2023. Heading and backing fire behaviours mediate the influence of fuels on wildfire energy. *International Journal of Wildland Fire* 32:1244–1261. https://doi.org/10.1071/WF22010.

Birch, J. D., J. A. Lutz, M. B. Dickinson, J. Franklin, A. J. Larson, M. E. Swanson, and J. R. Miesel. 2025. Small-scale fire refugia increase soil bacterial and fungal richness and increase community cohesion nine years after fire. *Science of the Total Environment* 966 : 178677. https://doi.org/10.1016/j.scitotenv.2025.178677.

Birch, J. D., J. R. Miesel, E. K. L. Batista, and M. B. Dickinson. 2026. Overstory retention in a managed mixed-conifer stand limits cheatgrass invasion after wildfire. *Fire Ecology*. https://doi.org/10.1186/s42408-025-00445-5.

Bradshaw, K. E. 1941. Field characters distinguishing *Pinus ponderosa* and *Pinus jeffreyi*. *Madroño* 6:15–18.

Bradshaw, L., McCormick, E., 2000. *FireFamily Plus user's guide, version 2.0. Gen. Tech. Rep. RMRS-GTR-67*. Ogden, UT: US Department of Agriculture, Forest Service, Rocky Mountain Research Station. 67.

Brodie, E. G., E. E. Knapp, A. M. Latimer, H. D. Safford, M. Vossmer, and S. M. Bisbing. 2023. The century-long shadow of fire exclusion: Historical data reveal early and lasting effects of fire regime change on contemporary forest composition. *Forest Ecology and Management* 539 : 121011. https://doi.org/10.1016/j.foreco.2023.121011.

Brodie, E. G., E. E. Knapp, W. R. Brooks, S. A. Drury, and M. W. Ritchie. 2024. Forest thinning and prescribed burning treatments reduce wildfire severity and buffer the impacts of severe fire weather. *Fire Ecology* 20:17. https://doi.org/10.1186/s42408-023-00241-z.

Brown, J., 1974. *Handbook for inventorying downed woody material*. In, USDA Forest Service General Technical Report, Intermountain Forest and Range Experiment Station, Ogden, UT, p. 24 pp.

Burgan, R. E., and R. C. Rothermel. 1984. *Behave: Fire behavior prediction and fuel modeling system, fuel subsystem*. US Department of Agriculture, Forest Service, Intermountain Forest and Range Experiment Station.

Butler, B. W., and M. B. Dickinson. 2010. Tree injury and mortality in fires: Developing process-based models. *Fire Ecology* 6:55–79. https://doi.org/10.4996/fireecology.0601055.

Chojnacky, D. C., L. S. Heath, and J. C. Jenkins. 2013. Updated generalized biomass equations for North American tree species. *Forestry: An International Journal of Forest Research* 87:129–151. https://doi.org/10.1093/forestry/cpt053.

Clarke, H., R. H. Nolan, V. R. De Dios, R. Bradstock, A. Griebel, S. Khanal, and M. M. Boer. 2022. Forest fire threatens global carbon sinks and population centres under rising atmospheric water demand. *Nature Communications* 13:7161. https://doi.org/10.1038/s41467-022-34966-3.

Conrad, O., B. Bechtel, M. Bock, H. Dietrich, E. Fischer, L. Gerlitz, J. Wehberg, V. Wichmann, and J. Böhner. 2015. System for automated geoscientific analyses (SAGA) v. 2.1.4. *Geosci. Model Dev.* 8:1991–2007. https://doi.org/10.5194/gmd-8-1991-2015.

Coppoletta, M., K. E. Merriam, and B. M. Collins. 2016. Post-fire vegetation and fuel development influences fire severity patterns in reburns. *Ecological Applications* 26:686–699. https://doi.org/10.1890/15-0225.

Cousins, S. J. M., J. J. Battles, J. E. Sanders, and R. A. York. 2015. Decay patterns and carbon density of standing dead trees in California mixed conifer forests. *Forest Ecology and Management* 353:136–147. https://doi.org/10.1016/j.foreco.2015.05.030.

Cruz, M. G., M. E. Alexander, and R. H. Wakimoto. 2004. Modeling the likelihood of crown fire occurrence in conifer forest stands. *Forest Science* 50:640–658. https://doi.org/10.1093/forestscience/50.5.640.

Dodge, J. M., E. K. Strand, A. T. Hudak, B. C. Bright, D. H. Hammond, and B. A. Newingham. 2019. Short- and long-term effects of ponderosa pine fuel treatments intersected by the Egley Fire Complex, Oregon, USA. *Fire Ecology* 15:40. https://doi.org/10.1186/s42408-019-0055-7.

Eidenshink, J., B. Schwind, K. Brewer, Z.-L. Zhu, B. Quayle, and S. Howard. 2007. A project for monitoring trends in burn severity. *Fire Ecology* 3:3–21. https://doi.org/10.4996/fireecology.0301003.

Evans, J.S., Ram, K., 2015. *spatialEco*. 1.3.7. https://cran.r-project.org/package=spatialEco

Fire Behavior Assessment Team, 2022. *FBAT 2022 measurement protocols*. In. United States Department of Agriculture.

Franklin, J. F., H. H. Shugart, and M. E. Harmon. 1987. Tree death as an ecological process. *BioScience* 37:550–556. https://doi.org/10.2307/1310665.

Furniss, T. J., A. J. Larson, V. R. Kane, and J. A. Lutz. 2020. Wildfire and drought moderate the spatial elements of tree mortality. *Ecosphere* 11 : e03214. https://doi.org/10.1002/ecs2.3214.

Germain, S. J., and J. A. Lutz. 2024. Stand diversity increases pine resistance and resilience to compound disturbance. *Fire Ecology* 20:53. https://doi.org/10.1186/s42408-024-00283-x.

Goforth, B. R., and R. A. Minnich. 2008. Densification, stand-replacement wildfire, and extirpation of mixed conifer forest in Cuyamaca Rancho State Park, southern California. *Forest Ecology and Management* 256:36–45. https://doi.org/10.1016/j.foreco.2008.03.032.

Goulden, M. L., and R. C. Bales. 2019. California forest die-off linked to multi-year deep soil drying in 2012–2015 drought. *Nature Geoscience* 12:632–637. https://doi.org/10.1038/s41561-019-0388-5.

Hagmann, R. K., P. F. Hessburg, S. J. Prichard, N. A. Povak, P. M. Brown, P. Z. Fulé, R. E. Keane, E. E. Knapp, J. M. Lydersen, K. L. Metlen, M. J. Reilly, A. J. Sánchez Meador, S. L. Stephens, J. T. Stevens, A. H. Taylor, L. L. Yocom, M. A. Battaglia, D. J. Churchill, L. D. Daniels, D. A. Falk, P. Henson, J. D. Johnston, M. A. Krawchuk, C. R. Levine, G. W. Meigs, A. G. Merschel, M. P. North, H. D. Safford, T. W. Swetnam, and A. E. M. Waltz. 2021. Evidence for widespread changes in the structure, composition, and fire regimes of western North American forests. *Ecological Applications* 31 : e02431. https://doi.org/10.1002/eap.2431.

Hall, S. A., I. C. Burke, and N. T. Hobbs. 2006. Litter and dead wood dynamics in ponderosa pine forests along a 160-year chronosequence. *Ecological Applications* 16:2344–2355. https://doi.org/10.1890/1051-0761(2006)016[2344:LADWDI]2.0.CO;2.

Harmon, M.E., Woodall, C.W., Fasth, B., Sexton, J., 2008. *Woody detritus density and density reduction factors for tree species in the United States: a synthesis* USDA For. Serv. Gen. Tech. Rep. NRS-29.

Harris, L. B., S. A. Drury, and A. H. Taylor. 2021. Strong legacy effects of prior burn severity on forest resilience to a high-severity fire. *Ecosystems* 24:774–787. https://doi.org/10.1007/s10021-020-00548-x.

Hill, A.P., Nolan, C.J., Hemes, K.S., Cambron, T.W., Field, C.B., 2023. *Low-elevation conifers in California's Sierra Nevada are out of equilibrium with climate* PNAS Nexus 2. https://doi.org/10.1093/pnasnexus/pgad004

Hood, S. M., J. M. Varner, P. van Mantgem, and C. A. Cansler. 2018. Fire and tree death: Understanding and improving modeling of fire-induced tree mortality. *Environmental Research Letters* 13 : 113004. https://doi.org/10.1088/1748-9326/aae934.

Hurteau, M. D., M. J. Goodwin, C. Marsh, H. S. Zald, B. Collins, M. Meyer, and M. P. North. 2024. Managing fire-prone forests in a time of decreasing carbon carrying capacity. *Frontiers in Ecology and the Environment* 22 : e2801. https://doi.org/10.1002/fee.2801.

Jenkins, J. C., D. C. Chojnacky, L. S. Heath, and R. A. Birdsey. 2003. National-scale biomass estimators for United States tree species. *Forest Science* 49:12–35. https://doi.org/10.1093/forestscience/49.1.12.

Jenkins, M. J., J. B. Runyon, C. J. Fettig, W. G. Page, and B. J. Bentz. 2013. Interactions among the Mountain Pine Beetle, fires, and fuels. *Forest Science* 60:489–501. https://doi.org/10.5849/forsci.13-017.

Johnson, E. A. 1996. *Fire and vegetation dynamics: Studies from The North American Boreal Forest*. Cambridge, UK: Cambridge University Press.

Johnstone, J. F., C. D. Allen, J. F. Franklin, L. E. Frelich, B. J. Harvey, P. E. Higuera, M. C. Mack, R. K. Meentemeyer, M. R. Metz, G. L. Perry, T. Schoennagel, and M. G. Turner. 2016. Changing disturbance regimes, ecological memory, and forest resilience. *Frontiers in Ecology and the Environment* 14:369–378. https://doi.org/10.1002/fee.1311.

Kassambara, A., 2023. *ggpubr: 'ggplot2' based publication ready plots* Version 0.4.0. https://cran.r-project.org/package=ggpubr.

Keen, R. M., S. L. Voelker, S.-Y.S. Wang, B. J. Bentz, M. L. Goulden, C. R. Dangerfield, C. C. Reed, S. M. Hood, A. Z. Csank, T. E. Dawson, A. G. Merschel, and C. J. Still. 2022. Changes in tree drought sensitivity provided early warning signals to the California drought and forest mortality event. *Global Change Biology* 28:1119–1132. https://doi.org/10.1111/gcb.15973.

Kelly, M., B. Allen-Diaz, and N. Kobzina. 2005. Digitization of a historic dataset: The Wieslander California Vegetation Type Mapping Project. *Madroño* 52:191–201. https://doi.org/10.3120/0024-9637(2005)52[191:DOAHDT]2.0.CO;2.

Kelly, M., K.-I. Ueda, and B. Allen-Diaz. 2008. Considerations for ecological reconstruction of historic vegetation: Analysis of the spatial uncertainties in the California Vegetation Type Map dataset. *Plant Ecology* 194:37–49. https://doi.org/10.1007/s11258-007-9273-1.

LANDFIRE, 2020. *Biophysical Settings, LANDFIRE 2.0.0. In: U.S. Department of the Interior, G.S., and U.S. Department of Agriculture (Ed.)*. U.S. Department of the Interior, Geological Survey, and U.S. Department of Agriculture. from https://www.landfire.gov/data/FullExtentDownloads. Accessed Jan 2023.

Liu, Z., and M. C. Wimberly. 2016. Direct and indirect effects of climate change on projected future fire regimes in the Western United States. *Science of the Total Environment* 542:65–75. https://doi.org/10.1016/j.scitotenv.2015.10.093.

Liu, Y., S. Goodrick, and W. Heilman. 2014. Wildland fire emissions, carbon, and climate: Wildfire–climate interactions. *Forest Ecology and Management* 317:80–96. https://doi.org/10.1016/j.foreco.2013.02.020.

Lutz, J. A., S. Struckman, T. J. Furniss, J. D. Birch, L. L. Yocom, and D. J. McAvoy. 2021. Large-diameter trees, snags, and deadwood in southern Utah, USA. *Ecological Processes* 10 : 9. https://doi.org/10.1186/s13717-020-00275-0.

Maringer, J., D. Ascoli, N. Küffer, S. Schmidtlein, and M. Conedera. 2016. What drives European beech (*Fagus sylvatica* L.) mortality after forest fires of varying severity? *Forest Ecology and Management* 368:81–93. https://doi.org/10.1016/j.foreco.2016.03.008.

Martin, A. R., M. Doraisami, and S. C. Thomas. 2018. Global patterns in wood carbon concentration across the world's trees and forests. *Nature Geoscience* 11:915–920. https://doi.org/10.1038/s41561-018-0246-x.

Miesel, J., A. Reiner, C. Ewell, B. Maestrini, and M. Dickinson. 2018. Quantifying changes in total and pyrogenic carbon stocks across fire severity gradients using active wildfire incidents. *Frontiers in Earth Science*. https://doi.org/10.3389/feart.2018.00041.

Milborrow, S., 2022. *Plotmo: plot a model's residuals, response, and partial dependence plots* 3.6.2. https://CRAN.R-project.org/package=plotmo.

Miller, J. D., and A. E. Thode. 2007. Quantifying burn severity in a heterogeneous landscape with a relative version of the delta Normalized Burn Ratio (dNBR). *Remote Sensing of Environment* 109:66–80. https://doi.org/10.1016/j.rse.2006.12.006.

Monitoring Trends in Burn Severity, 2023. *Burn severity database. In: US Department of Agriculture* U.G.S. (Ed.).

Nolan, R. H., L. Collins, R. K. Gibson, S. A. Samson, K. T. Rolls, K. Milner, B. E. Medlyn, O. F. Price, A. Griebel, B. Choat, M. Jiang, and M. M. Boer. 2022. The carbon cost of the 2019–20 Australian fires varies with fire severity and forest type. *Global Ecology and Biogeography* 31:2131–2146. https://doi.org/10.1111/geb.13548.

North, M. P., R. A. York, B. M. Collins, M. D. Hurteau, G. M. Jones, E. E. Knapp, L. Kobziar, H. McCann, M. D. Meyer, S. L. Stephens, R. E. Tompkins, and C. L.

Tubbesing. 2021. Pyrosilviculture needed for landscape resilience of dry Western United States forests. *Journal of Forestry* 119:520–544. https://doi.org/10.1093/jofore/fvab026.
Oksanen, J., Simpson, G., Blanchet, F., Kindt, R., Legendre, P., Minchin, P., O'hara, R., Solymos, P., Stevens, M., Szoecs, E., 2023. *vegan: community ecology package* Version 2.6–4. https://cran.r-project.org/web//packages//vegan/index.html
Page, W. G., M. E. Alexander, and M. J. Jenkins. 2013. Wildfire's resistance to control in mountain pine beetle-attacked lodgepole pine forests. *The Forestry Chronicle* 89:783–794. https://doi.org/10.5558/tfc2013-141.
Parsons, D. J., and S. H. DeBenedetti. 1979. Impact of fire suppression on a mixed-conifer forest. *Forest Ecology and Management* 2:21–33. https://doi.org/10.1016/0378-1127(79)90034-3.
Peterson, D. W., E. K. Dodson, and R. J. Harrod. 2023. Snag decomposition following stand-replacing wildfires alters wildlife habitat use and surface woody fuels through time. *Ecosphere* 14 : e4635. https://doi.org/10.1002/ecs2.4635.
Pimm, S. L. 1984. The complexity and stability of ecosystems. *Nature* 307:321–326. https://doi.org/10.1038/307321a0.
Prichard, S. J., D. L. Peterson, and K. Jacobson. 2010. Fuel treatments reduce the severity of wildfire effects in dry mixed conifer forest, Washington, USA. *Canadian Journal of Forest Research* 40:1615–1626. https://doi.org/10.1139/x10-109.
R Core Team, 2023. R: A language and environment for statistical computing. *R Foundation for Statistical Computing.Version* 4.2.2. https://www.r-project.org/
R Studio Team, 2023. *Studio: Integrated Development for R*. Posit.Version 2023.06.02. https://posit.co/downloads/.
Rao, K., A. P. Williams, N. S. Diffenbaugh, M. Yebra, and A. G. Konings. 2022. Plant-water sensitivity regulates wildfire vulnerability. *Nature Ecology & Evolution* 6:332–339. https://doi.org/10.1038/s41559-021-01654-2.
Reed, C.C., Hood, S.M., 2023. *Nonstructural carbohydrates explain post-fire tree mortality and recovery patterns* Tree Physiology 44. https://doi.org/10.1093/treephys/tpad155
Régnière, J., Saint-Amant, R., Béchard, A., Moutaoufik, A., 2018. *BioSIM 11 User's Manual. Update of Information Report LAU-X-137*. Natural Resources Canada, Canadian Forest Service, Laurentian Forestry Centre.
Rein, G. 2016. Smoldering combustion. In *SFPE handbook of fire protection engineering*, 581–603.
Reiner, A.L., Ewell, C.M., Fites-Kaufman, J.A., Dailey, S.N., Noonan-Wright, E.K., Norman, T.P., Vaillant, N.M., Dickinson, M.B., Morgan, C., Courson, M., Campbell, M., 2021. *Fire behavior assessment team: in-fire videos*. In: United States Department of Agriculture (Ed.), Forest Service Research Data Archive. https://doi.org/10.2737/RDS-2021-0069
Restaino, C., D. J. N. Young, B. Estes, S. Gross, A. Wuenschel, M. Meyer, and H. Safford. 2019. Forest structure and climate mediate drought-induced tree mortality in forests of the Sierra Nevada, USA. *Ecological Applications* 29 : e01902. https://doi.org/10.1002/eap.1902.
Ritchie, M. W., E. E. Knapp, and C. N. Skinner. 2013. Snag longevity and surface fuel accumulation following post-fire logging in a ponderosa pine dominated forest. *Forest Ecology and Management* 287:113–122. https://doi.org/10.1016/j.foreco.2012.09.001.
Roccaforte, J. P., P. Z. Fulé, W. W. Chancellor, and D. C. Laughlin. 2012. Woody debris and tree regeneration dynamics following severe wildfires in Arizona ponderosa pine forests. *Canadian Journal of Forest Research* 42:593–604. https://doi.org/10.1139/x2012-010.
Safford, H. D., and J. T. Stevens. 2017. *Natural range of variation for yellow pine and mixed-conifer forests in the Sierra Nevada, southern Cascades, and Modoc and Inyo National Forests*. USA: California.
Schmitt, A., R. Trouvé, I. Seynave, and F. Lebourgeois. 2020. Decreasing stand density favors resistance, resilience, and recovery of *Quercus petraea* trees to a severe drought, particularly on dry sites. *Annals of Forest Science* 77 : 52. https://doi.org/10.1007/s13595-020-00959-9.
Serra-Diaz, J. M., C. Maxwell, M. S. Lucash, R. M. Scheller, D. M. Laflower, A. D. Miller, A. J. Tepley, H. E. Epstein, K. J. Anderson-Teixeira, and J. R. Thompson. 2018. Disequilibrium of fire-prone forests sets the stage for a rapid decline in conifer dominance during the 21st century. *Scientific Reports* 8 : 6749. https://doi.org/10.1038/s41598-018-24642-2.
Shive, K. L., A. Wuenschel, L. J. Hardlund, S. Morris, M. D. Meyer, and S. M. Hood. 2022. Ancient trees and modern wildfires: Declining resilience to wildfire in the highly fire-adapted Giant Sequoia. *Forest Ecology and Management* 511 : 120110. https://doi.org/10.1016/j.foreco.2022.120110.
Steel, Z. L., H. D. Safford, and J. H. Viers. 2015. The fire frequency-severity relationship and the legacy of fire suppression in California forests. *Ecosphere* 6 : art8. https://doi.org/10.1890/ES14-00224.1.
Steel, Z. L., G. M. Jones, B. M. Collins, R. Green, A. Koltunov, K. L. Purcell, S. C. Sawyer, M. R. Slaton, S. L. Stephens, P. Stine, and C. Thompson. 2023. Mega-disturbances cause rapid decline of mature conifer forest habitat in California. *Ecological Applications* 33 : e2763. https://doi.org/10.1002/eap.2763.
Stephens, S. L., J. T. Stevens, B. M. Collins, R. A. York, and J. M. Lydersen. 2018. Historical and modern landscape forest structure in fir (*Abies*)-dominated mixed conifer forests in the northern Sierra Nevada, USA. *Fire Ecology* 14 : 7. https://doi.org/10.1186/s42408-018-0008-6.
Stephens, S. L., A. A. Bernal, B. M. Collins, M. A. Finney, C. Lautenberger, and D. Saah. 2022. Mass fire behavior created by extensive tree mortality and high tree density not predicted by operational fire behavior models in the southern Sierra Nevada. *Forest Ecology and Management* 518 : 120258. https://doi.org/10.1016/j.foreco.2022.120258.
Stevens-Rumann, C. S., K. B. Kemp, P. E. Higuera, B. J. Harvey, M. T. Rother, D. C. Donato, P. Morgan, and T. T. Veblen. 2018. Evidence for declining forest resilience to wildfires under climate change. *Ecology Letters* 21:243–252. https://doi.org/10.1111/ele.12889.
Stockstad, D.S., 1979. *Spontaneous and piloted ignition of rotten wood*. In. Intermountain Forest and Range Experiment Station, USDA Forest Service, Missoula, MT, USA, p. 12.
Taylor, A. H., and C. N. Skinner. 2003. Spatial patterns and controls on historical fire regimes and forest structure in the Klamath Mountains. *Ecological Applications* 13:704–719. https://doi.org/10.1890/1051-0761(2003)013[0704:SPACOH]2.0.CO;2.
Thompson, D. K., M.-A. Parisien, J. Morin, K. Millard, C. P. S. Larsen, and B. N. Simpson. 2017. Fuel accumulation in a high-frequency boreal wildfire regime: From wetland to upland. *Canadian Journal of Forest Research* 47:957–964. https://doi.org/10.1139/cjfr-2016-0475.
Tortorelli, C. M., A. M. Latimer, and D. J. N. Young. 2024. Moderating effects of past wildfire on reburn severity depend on climate and initial severity in Western US forests. *Ecological Applications* 34 : e3023. https://doi.org/10.1002/eap.3023.
Turco, M., J. T. Abatzoglou, S. Herrera, Y. Zhuang, S. Jerez, D. D. Lucas, A. AghaKouchak, and I. Cvijanovic. 2023. Anthropogenic climate change impacts exacerbate summer forest fires in California. *Proceedings of the National Academy of Sciences* 120 : e2213815120. https://doi.org/10.1073/pnas.2213815120.
United States Geological Survey, 2020. *USGS National Elevation Dataset*. In: United States Department of the Interior (Ed.). from https://apps.nationalmap.gov/downloader/#/. Accessed Jan 2023.
United States Forest Service, 2024. *Forest activity tracking system (FACTS)*. In: United States Department of Agriculture (Ed.). from https://data.fs.usda.gov/geodata/edw/datasets.php?xmlKeyword=FACTS+common+attributes. Accessed Jan 2023.
Van Wagtendonk, J. W., J. M. Benedict, and W. M. Sydoriak. 1998. Fuel bed characteristics of Sierra Nevada conifers. *Western Journal of Applied Forestry* 13:73–84. https://doi.org/10.1093/wjaf/13.3.73.
Vernon, M. J., R. L. Sherriff, P. van Mantgem, and J. M. Kane. 2018. Thinning, tree-growth, and resistance to multi-year drought in a mixed-conifer forest of Northern California. *Forest Ecology and Management* 422:190–198. https://doi.org/10.1016/j.foreco.2018.03.043.
Vicente-Serrano, S. M., S. Beguería, and J. I. López-Moreno. 2010. A multiscalar drought index sensitive to global warming: The Standardized Precipitation Evapotranspiration Index. *Journal of Climate* 23:1696–1718. https://doi.org/10.1175/2009JCLI2909.1.
Volkova, L., K. I. Paul, S. H. Roxburgh, and C. J. Weston. 2022. Tree mortality and carbon emission as a function of wildfire severity in south-eastern Australian temperate forests. *Science of the Total Environment* 853 : 158705. https://doi.org/10.1016/j.scitotenv.2022.158705.
Wagner, C.v., 1972. *Heat of combustion, heat yield and fire behaviour*. In, Information Report, Petawawa Forest Experiment Station, Canada, p. 7 pp.
Wang, T., A. Hamann, D. Spittlehouse, and C. Carroll. 2016. Locally downscaled and spatially customizable climate data for historical and future periods for North America. *PLoS ONE* 11 : e0156720. https://doi.org/10.1371/journal.pone.0156720.

Wickham, H. 2016. *ggplot2: Elegant graphics for data analysis*. Springer International Publishing. https://doi.org/10.1007/978-3-319-24277-4_9.
Williams, C. A., H. Gu, R. MacLean, J. G. Masek, and G. J. Collatz. 2016. Disturbance and the carbon balance of US forests: A quantitative review of impacts from harvests, fires, insects, and droughts. *Global and Planetary Change* 143:66–80. https://doi.org/10.1016/j.gloplacha.2016.06.002.
Wood, S. N. 2010. Fast stable restricted maximum likelihood and marginal likelihood estimation of semiparametric generalized linear models. *Journal of the Royal Statistical Society Series B: Statistical Methodology* 73:3–36. https://doi.org/10.1111/j.1467-9868.2010.00749.x.
Wood, S.N., 2023. Mixed GAM computation vehicle with automatic smoothness estimations. 1.8-40. https://cran.r-project.org/package=mgcv.
Xu, R., T. Ye, W. Huang, X. Yue, L. Morawska, M. J. Abramson, G. Chen, P. Yu, Y. Liu, Z. Yang, Y. Zhang, Y. Wu, W. Yu, B. Wen, Y. Zhang, S. Hales, E. Lavigne, P. H. N. Saldiva, M. S. Z. S. Coelho, P. Matus, D. Roye, J. Klompmaker, M. Mistry, S. Breitner, A. Zeka, R. Raz, S. Tong, F. H. Johnston, J. Schwartz, A. Gasparrini, Y. Guo, and S. Li. 2024. Global, regional, and national mortality burden attributable to air pollution from landscape fires: A health impact assessment study. *The Lancet* 404:2447–2459. https://doi.org/10.1016/S0140-6736(24)02251-7.
Zhang, J., K. A. Finley, N. G. Johnson, and M. W. Ritchie. 2019. Lowering stand density enhances resiliency of ponderosa pine forests to disturbances and climate change. *Forest Science* 65:496–507. https://doi.org/10.1093/forsci/fxz006.

Publisher's Note